MUNC13-4 Protein Regulates the Oxidative Response and Is Essential for Phagosomal Maturation and Bacterial Killing in Neutrophils*[S]

Jlenia Monfregola[‡1], **Jennifer Linda Johnson**[‡], **Michael M. Meijler**[§], **Gennaro Napolitano**[‡2], and **Sergio Daniel Catz**[‡3]

From the ‡*Department of Molecular and Experimental Medicine, The Scripps Research Institute, La Jolla, California 92037 and* §*Department of Chemistry and National Institute for Biotechnology in the Negev, Ben-Gurion University of the Negev, Be'er-Sheva 84105, Israel*

Background: MUNC13-4 regulates vesicular trafficking, and its deficiency causes immunodeficiency in humans.
Results: MUNC13-4 regulates ROS production, phagosomal maturation, and bacterial killing in neutrophils.
Conclusion: MUNC13-4 is essential for the neutrophil-dependent innate immune response.
Significance: This study identifies MUNC13-4 as a potential target for therapeutic intervention during bacterial infections.

Neutrophils use diverse mechanisms to kill pathogens including phagocytosis, exocytosis, generation of reactive oxygen species (ROS), and neutrophil extracellular traps. These mechanisms rely on their ability to mobilize intracellular organelles and to deliver granular cargoes to specific cellular compartments or into the extracellular milieu, but the molecular mechanisms regulating vesicular trafficking in neutrophils are not well understood. MUNC13-4 is a RAB27A effector that coordinates exocytosis in hematopoietic cells, and its deficiency is associated with the human immunodeficiency familial hemophagocytic lymphohistiocytosis type 3. In this work, we have established an essential role for MUNC13-4 in selective vesicular trafficking, phagosomal maturation, and intracellular bacterial killing in neutrophils. Using neutrophils from *munc13-4* knock-out (KO) mice, we show that MUNC13-4 is necessary for the regulation of p22*phox*-expressing granule trafficking to the plasma membrane and regulates extracellular ROS production. MUNC13-4 was also essential for the regulation of intracellular ROS production induced by *Pseudomonas aeruginosa* despite normal trafficking of p22*phox*-expressing vesicles toward the phagosome. Importantly, in the absence of MUNC13-4, phagosomal maturation was impaired as observed by the defective delivery of azurophilic granules and multivesicular bodies to the phagosome. Significantly, this mechanism was intact in RAB27A KO neutrophils. Intracellular bacterial killing was markedly impaired in MUNC13-4 KO neutrophils. MUNC13-4-deficient cells showed a significant increase in neutrophil extracellular trap formation but were unable to compensate for the impaired bacterial killing. Altogether, these findings characterize novel functions of MUNC13-4 in the innate immune response of the neutrophil and have direct implications for the understanding of immunodeficiencies in patients with MUNC13-4 deficiency.

Neutrophils constitute the first line of cellular defense against bacterial and fungal infections and play a key role in the innate immune response to a broad range of pathogens. Neutrophils utilize several antimicrobial strategies including exocytosis-mediated release of antimicrobial molecules into the extracellular milieu (1), phagocytosis (2), and neutrophil extracellular trap (NET)[4] formation (3). The efficiency of pathogen killing by neutrophils through degranulation, phagocytosis, and NETs relies on the timely activation of neutrophil granular proteins (2, 4).

Granular secretory proteins are held in diverse neutrophil secretory organelles (5). Mature neutrophils contain four types of storage organelles: azurophilic granules, specific granules, gelatinase granules, and secretory vesicles (5). They also contain multivesicular bodies (MVBs) (6), which are formed by the endocytic pathway and are both exocytosable and able to fuse with the phagosome (7). Sequential mobilization of neutrophil organelles and the release of their cargoes into the extracellular milieu or into the intraphagosomal space are necessary events to mediate extracellular or intracellular killing, respectively. The release of granular proteins is also significant for the formation of neutrophil extracellular traps (4). Importantly, defects in granular proteins are associated with immunodeficiencies in mice and humans. For example, deficiencies in the azurophilic granule protein elastase, a strong antibacterial serine protease, or myeloperoxidase (MPO), the enzyme responsible for the formation of antibacterial oxidized halides, are

[1] A postdoctoral fellow of the American Heart Association.
[2] A fellow of the Cystinosis Research Foundation.
[3] To whom correspondence should be addressed: Dept. of Molecular and Experimental Medicine, The Scripps Research Inst., 10550 North Torrey Pines Rd., La Jolla, CA 92037. Tel.: 858-784-7932; Fax: 858-784-2054; E-mail: scatz@scripps.edu.

[4] The abbreviations used are: NET, neutrophil extracellular trap; ROS, reactive oxygen species; MVB, multivesicular body; MPO, myeloperoxidase; CGD, chronic granulomatous disease; fMLP, formyl-methionyl-leucyl-phenylalanine; LAMP1, lysosome-associated membrane protein 1; FHL3, familial hemophagocytic lymphohistiocytosis type 3; TIRF, total internal reflection fluorescence; XTT, 3,3'-[1{(phenylamino)carbonyl}-3,4-tetrazolium]-bis[4-methoxy-6-nitro]benzene sulfonic acid hydrate; WGA, wheat germ agglutinin.

associated with susceptibility to bacterial and fungal infections (8–10).

The bactericidal activity of neutrophils is also mediated by their ability to generate reactive oxygen species (ROS). In neutrophils, ROS production relies on the NADPH oxidase, a multisubunit enzymatic complex that is responsible for the monoelectronic reduction of oxygen to produce superoxide anion (O_2^-) (11). The production of O_2^- is directly associated with the microbicidal capacity of these cells because patients with chronic granulomatous disease (CGD), whose NADPH oxidase is inactive, suffer recurrent bacterial and fungal infections (12). The neutrophil NADPH oxidase complex is composed of the cytosolic factors $p47^{phox}$, $p67^{phox}$, and $p40^{phox}$; the membrane-associated flavocytochrome b_{558} (formed by the subunits $gp91^{phox}$ and $p22^{phox}$); and the accessory proteins Rac2 (13) and Rap1a (14–16). In unstimulated neutrophils, the oxidase is dissociated and inactive. In response to appropriate stimuli, the flavocytochrome b_{558} assembles with the cytosolic factors, generating a functional complex (14). Most subunits of the flavocytochrome b_{558} are associated with the membranes of intracellular specific and gelatinase granules, and only a small proportion is also present at the plasma membrane (17). Many soluble stimuli including the bacterially derived chemotactic peptide formyl-methionyl-leucyl-phenylalanine (fMLP) (18) and lipopolysaccharide (LPS) (19) are able to up-regulate the number of plasma membrane-associated NADPH oxidase subunits by inducing the mobilization of intracellular secretory organelles and promoting the fusion of granule membranes with the plasmalemma, thus increasing the oxidative activity in the milieu surrounding the neutrophil. In addition, during phagocytosis, flavocytochrome b_{558}-containing granules fuse with the phagosome, and the oxidase is assembled at phagosomal membranes (20–22). Equally important, azurophilic granules and multivesicular bodies are able to fuse with the phagosomal membrane in a sequential manner in a process referred to as phagosome maturation (23, 24). Thus, myeloperoxidase and serine proteases are released from azurophilic granules into the phagosome to mediate the formation of antibacterial HOCl at the expense of H_2O_2 and to degrade bacterial materials, respectively. Lysosome-associated membrane protein 1 (LAMP1), which in neutrophils localizes at MVBs (6), is also considered an important factor for efficient phagosomal maturation (24). From this, it is clear that granule trafficking and fusion are essential for the neutrophil innate immune response, but the molecular mechanisms regulating these processes are not fully characterized.

The small GTPase RAB27A is a master organizer of vesicular trafficking and, together with its specific effectors, controls exocytosis in hematopoietic cells (25). In neutrophils, RAB27A controls azurophilic granule exocytosis and regulates the activation of the NADPH oxidase at the plasma membrane (26–28). The RAB27A effector MUNC13-4 is also involved in the regulation of granule exocytosis (27, 29, 30) and controls the priming of myeloperoxidase release in response to bacterial lipopolysaccharide (30), but its role in other neutrophil functions remains unknown. Importantly, defects in the *rab27a* or the *unc13-4* genes are associated with immunodeficiencies in humans (31). For instance, RAB27A deficiency causes Griscelli

syndrome type 2, an immunodeficiency with partial albinism (32), whereas MUNC13-4 deficiency is the cause of human familial hemophagocytic lymphohistiocytosis type 3 (FHL3) (33). Both RAB27A and MUNC13-4 deficiencies are associated with malfunction of cytotoxic T lymphocytes, natural killer cells, and neutrophils, and patients with Griscelli syndrome type 2 and FHL3 suffer an accelerated phase (hemophagocytic lymphohistiocytic syndrome) initiated by recurrent and often fatal viral and bacterial infections (34).

In neutrophils, MUNC13-4 regulates exocytosis of azurophilic (30) and tertiary (29) granules, but the increased susceptibility of patients with FHL3 to bacterial infections (34) suggests further defects in neutrophil function. Possible roles for MUNC13-4 in the control of the secretion of other neutrophil granules, ROS production, phagocytosis maturation, or NET formation have not been explored. In this work, using neutrophils from MUNC13-4-deficient mice, we show that MUNC13-4 plays a previously unrecognized fundamental role in the regulation of neutrophil phagosome maturation and ROS production.

EXPERIMENTAL PROCEDURES

Experimental Animal Models—Our experiments utilized C57BL/6 *munc13-4*^*jinx/jinx*^ mice (here referred to as *munc13-4* KO mice) (35), *ashen* mice (C57BL/6-*rab27a*^*ash/ash*^) (36), and their parental strain, C57BL/6 (wild type). The *munc13-4* KO mouse model was generated by random germ line mutagenesis using the alkylating agent *N*-ethyl-*N*-nitrosourea (35). Based on Western blot analysis, we have previously established that *munc13-4* KO mice have a MUNC13-4-null phenotype (27). The *munc13-4* KO mice were maintained as a homozygous stock for use in these studies. *rab27a*^*ash/ash*^ (RAB27A KO) mice that contain a splicing mutation in the *rab27a* gene have been extensively utilized for the study of RAB27A deficiency and were described previously (36). Mice (6–12 weeks old) were maintained in a pathogen-free environment and had access to food and water *ad libitum*. The *gp91*^*phox*^ KO mice were contributed by Dr. Josh Fierer (University of California, San Diego) and were described previously (37, 38). All animal studies were performed in compliance with the United States Department of Health and Human Services Guide for the Care and Use of Laboratory Animals. All studies were conducted according to National Institutes of Health and institutional guidelines and with approval of the animal review board at The Scripps Research Institute.

Isolation of Neutrophils—Bone marrow-derived neutrophils were isolated using a Percoll gradient fractionation system as described (39). For neutrophil isolation, a three-layer Percoll gradient was used (52, 62, and 78%). Neutrophils were isolated from the 62 to 78% interface, washed, and used in all our assays. Human neutrophils were isolated from normal donor's blood by Ficoll density centrifugation as described previously (40). Cell fractionation assays using sucrose gradients were performed exactly as depicted before (26).

ROS Production—Neutrophil ROS production was measured using the chemiluminescence reactions mediated by luminol or isoluminol as described previously (22, 28). For the detection of extracellular ROS, 3×10^5 neutrophils were resuspended in

RPMI 1640 medium in the presence of isoluminol and horseradish peroxidase (6.58 units/ml). Neutrophils were stimulated with fMLP (10 μM), and chemiluminescence was continuously monitored for up to 20 min at 37 °C using an EG&G Berthold microplate luminometer. Where indicated, neutrophils were preincubated with LPS (10 ng/ml) for 30 min before fMLP stimulation. For the analysis of intracellular ROS production, neutrophils were stimulated with serum-opsonized *Pseudomonas aeruginosa* strain PAK kindly contributed by Dr. S. Lory at Harvard University. Bacteria were utilized at a ratio of 1:10 (neutrophils/bacteria). In other experiments, neutrophils were stimulated with phorbol 12-myristate 13-acetate (0.1 μg/ml), and luminol-dependent chemiluminescence was continuously monitored for 20 min at 37 °C. Where indicated, the cells were incubated in the presence of superoxide dismutase (300 units/ml) or cytochalasin D (10 μg/ml) for 10 min before stimulation.

Total Internal Reflection Fluorescence (TIRF) Microscopy Analysis—Wild type and MUNC13-4 KO murine neutrophils were seeded in 8-well plates with bottom coverglass (number 1.5 borosilicate coverglass, Lab-Tek, Nunc). The cells were fixed with 4% paraformaldehyde, permeabilized with 0.02% saponin, and blocked with a solution of 2% BSA in PBS. The samples were incubated with primary antibodies overnight at 4 °C in the presence of 0.02% saponin and blocking agents and subsequently labeled using Alexa Fluor 488- or 594-conjugated secondary antibodies (Invitrogen). The cells were stored in unsolidified water-based mounting medium (refractive index, 1.37) or PBS until analyzed. TIRF microscopy experiments were performed using a 100× 1.45 numerical aperture TIRF objective (Nikon) on a Nikon TE2000U microscope custom modified with a TIRF illumination module as described (30). Images were acquired on a 14-bit, cooled charge-coupled device camera (Hamamatsu) controlled through NIS-Elements software. The images were recorded using 300–500-ms exposures depending on the fluorescence intensity of the sample. Images were analyzed using ImageJ software (version 1.43) and quantified using Quantity One analysis software (Bio-Rad).

Immunofluorescence and Confocal Microscopy Analysis—Wild type and MUNC13-4 KO murine neutrophils were seeded on untreated number 1.5 borosilicate coverglasses (Corning). Where indicated, neutrophils were stimulated with fMLP (10 μM) or exposed to rhodamine-labeled *P. aeruginosa* for the indicated time at 37 °C, then fixed with 4% paraformaldehyde, permeabilized with 0.02% saponin, and blocked with 2% BSA in PBS. Samples were labeled with the indicated primary antibodies overnight at 4 °C in the presence of 0.02% saponin and 2% BSA. Samples were washed and subsequently incubated with the appropriate combinations of Alexa Fluor (488, 594, or 633)-conjugated donkey anti-rabbit, anti-rat, or anti-mouse secondary antibodies (Invitrogen). To stain the neutrophil extracellular traps, samples were incubated with 4′,6-diamidino-2-phenylindole dihydrochloride (DAPI) for 15 min at 21 °C and gently washed with PBS. Cells were stored in Fluoromount-G (Southern Biotechnology, Birmingham, AL) and analyzed using a Zeiss LSM 710 laser-scanning confocal microscope attached to a Zeiss Observer Z1 microscope using the 63× or 40× oil Plan Apo, 1.4 numerical aperture infinity-cor-

rected optics at 21 °C. For visualization, fluorescence associated with Alexa Fluor 594-labeled secondary antibody was excited using the 543-nm laser line and collected using a standard Texas Red filter. Fluorescence associated with Alexa Fluor 488-labeled secondary antibodies was visualized using the 488-nm laser line and collected using a standard FITC filter set. Fluorescence associated with Alexa Fluor 633-labeled secondary antibodies was visualized using the 632-nm laser line and collected using a standard filter set. Images were collected using ZEN-LSM software and processed using ImageJ and Adobe Photoshop CS4.

Quantification of NETs—NETs were quantified using SYTOX Green as described previously (41). To this end, neutrophils were seeded into 96-well plates (1×10^6/well) and stimulated with *P. aeruginosa* in a 3:1 ratio (bacteria/neutrophil) in the presence or absence of DNase I (100 units/ml) for 3 h at 37 °C. Next, the cell-impermeable nucleic acid stain SYTOX Green (Invitrogen) was added to a final concentration of 5 μM. Unstimulated neutrophils and bacteria alone were always included as controls. The samples were analyzed for fluorescence intensity (485-nm excitation/527-nm emission) using a SpectraMax Gemini EM spectrofluorometer (Molecular Devices). In some experiments, NET production was quantified by confocal microscopy. To this end, wild type and MUNC13-4 KO murine neutrophils were seeded on an untreated coverglass, stimulated, fixed, and incubated with DAPI for 15 min at 21 °C. Samples were analyzed by confocal microscopy using a Zeiss LSM 710 laser-scanning confocal microscope attached to a Zeiss Observer Z1 microscope using the 40× oil Plan Apo, 1.4 numerical aperture infinity-corrected optics at 21 °C. Images were processed using ImageJ, and NETs were counted manually from 10 fields for each experimental condition. The percentage of NET-producing cells was calculated by dividing the number of NET-producing cells in each field by the total number of cells in the same field for wild type and MUNC13-4 KO neutrophils.

Labeling of Bacteria—*P. aeruginosa* strain PAK was used for all studies and was grown overnight in Luria broth medium at 37 °C with vigorous aeration. Prior to experiments, bacteria were subcultured at 37 °C and grown to logarithmic growth from an overnight culture. Subsequently, the bacteria were collected by centrifugation, washed twice in PBS, and resuspended in PBS to an A_{600} of 1 (*i.e.* 1×10^9 bacteria/ml). For labeling, the bacteria were incubated overnight at 4 °C in the presence of freshly prepared 50 μM tetramethylrhodamine mixture (33.3 mM tetramethylrhodamine, 33.3 mM 1-ethyl-3-(3-dimethylaminopropyl) carbodiimide hydrochloride), and 33.3 mM *N*-hydroxysuccinimide). Bacteria were washed twice with PBS, viability was checked microscopically, and bacteria were immediately used in phagocytosis assays.

Phagocytosis Assay—Phagocytosis was measured using tetramethylrhodamine-labeled live *P. aeruginosa.* Briefly, serum-opsonized fluorescently labeled live bacteria were added to 2×10^6 neutrophils at a ratio of 3:1 (bacteria/neutrophil) in a final volume of 0.3 ml of PBS. The samples were incubated for 1 h at 4 °C for synchronization and subsequently incubated for 15, 45, 60, and 180 min at 37 °C. A trypan blue quenching solution was prepared by diluting the trypan blue stock solu-

tion (0.4%) 1:10 in PBS buffer and added to the samples. Samples were washed with PBS, fixed with 4% paraformaldehyde, used for immunofluorescence, and analyzed by confocal microscopy.

Gel Electrophoresis and Western Blotting—Proteins were separated by gel electrophoresis using NuPAGE gels and MOPS buffer (Invitrogen). Proteins were transferred onto nitrocellulose membranes for 180 min at 60 V and 4 °C. The membranes were blocked with PBS containing 5% (w/v) blotting grade non-fat dry milk blocker (Bio-Rad) and 0.05% (w/v) Tween 20. Proteins were detected by probing the membranes with the indicated primary antibodies at appropriate dilutions and using a detection system consisting of horseradish peroxidase (HRP)-conjugated secondary antibodies (Bio-Rad) and chemiluminescent substrates (Thermo Fisher Scientific) visualized using Hyperfilm films (Amersham Biosciences).

Chromogenic Bacterial Killing Assay—Bacterial killing assays using mouse neutrophils were performed by adapting a previously described killing assay in suspension (42) to a chromogenic quantitative detection of live bacteria (43). Briefly, *P. aeruginosa* strain PAK was subcultured at 37 °C to logarithmic growth from an overnight culture by adding 1 ml of this culture to 30 ml of Luria broth, and this new culture was grown for an extra 3 h. Subsequently, the bacteria were collected by centrifugation (3000 rpm for 5 min), washed twice in PBS, and resuspended in PBS to an A_{600} of 1. After opsonization (10% (v/v) pooled serum for 15 min at 37 °C), bacteria were added to 2×10^6 neutrophils in a ratio of 3:1 (bacteria/neutrophil) and incubated for 3 h with rotation at 37 °C. This ratio of bacteria/neutrophil was chosen based on the highest bone marrow-derived neutrophil-dependent killing of *P. aeruginosa* we observed under the experimental conditions described in this protocol. Reactions consisting of live bacteria incubated with heat-killed neutrophils were used as control. The reactions were diluted in water/NaOH (pH 11) and incubated for 5 min at 37 °C to lyse neutrophils. Bacteria were spun at 3000 rpm, resuspended in Luria broth medium, and incubated for an extra 1 h at 37 °C. After incubation, samples were seeded into 96-well plates, and 20 μl of a freshly made formazan dye (3,3′-[1{(phenylamino)-carbonyl}-3,4-tetrazolium]-bis[4-methoxy-6-nitro]benzene sulfonic acid hydrate (XTT)) substrate solution was added to each well as described previously (43). The substrate solution was prepared in phosphate-buffered saline containing XTT (0.5 mg/ml; Sigma). The plates were incubated at room temperature, and the A_{450} was measured at 0 and 30 min. The ability of wild type and MUNC13-4 KO neutrophils to kill extracellular live bacteria was measured by addition of XTT after the 3-h incubation time but without alkaline lysis. As XTT has a net negative charge and is largely cell-impermeable (44), this only detects extracellular bacteria. Color formation by bone marrow-derived neutrophils in the absence of bacteria under these assay conditions was insignificant (not shown). The percentage of bacterial survival was calculated by dividing the values obtained from each sample by the values measured in the respective control (bacteria plus heat-killed neutrophils) in wild type and MUNC13-4 KO cells.

Antibodies—The polyclonal antibody against p22^{phox} (NPP-1890) was raised in rabbits using the synthetic peptide CNPPPRPPAEARKKPSE, and its characterization is presented in supplemental Fig. S1. The generation and characterization of the anti-gp91^{phox} monoclonal antibody 18C7 were described previously (45). The rabbit polyclonal antibody raised against MUNC13-4 was described previously (27). We also used anti-CD35 (Santa Cruz Biotechnology, Santa Cruz, CA), anti-MPO (Hycult Biotech), and anti-LAMP1 (Santa Cruz Biotechnology).

RESULTS

MUNC13-4 Regulates the Number of p22^{phox}-expressing Granules at the Exocytic Active Zone—The neutrophil oxidative response is essential for the efficient bactericidal activity of these cells. Because exocytosis is considered an important factor for NADPH oxidase activation (18) and MUNC13-4 regulates exocytosis in neutrophils (29, 30), we sought to analyze a possible function for MUNC13-4 in ROS production regulation. First, we determined the subcellular distribution of MUNC13-4 in relationship to that of flavocytochrome b_{558} by cell fractionation and confocal microscopy. We found that endogenous MUNC13-4 colocalizes and cofractionates with organelles expressing gp91^{phox} and p22^{phox}, respectively (Fig. 1, *A* and *B*), which are generally accepted to exist solely as heterodimers in mature neutrophils (46). This suggested a possible role for MUNC13-4 in the regulation of flavocytochrome b_{558} trafficking.

MUNC13-4 regulates vesicular trafficking and has been proposed to regulate vesicular tethering (47), docking (30), and fusion (33) during exocytosis. To analyze whether the deficiency in MUNC13-4 is associated with abnormal distribution or mobilization of flavocytochrome b_{558}-expressing organelles, we utilized TIRF microscopy and analyzed the localization of flavocytochrome b_{558}-expressing granules in relationship to the plasma membrane in MUNC13-4 KO cells. In TIRF microscopy, imaging is confined to the cell surface such that it detects fluorescence events within ~100 nm of the coverslip, allowing the analysis of processes that take place in close proximity to the plasma membrane (48), hereafter referred to as the exocytic active zone (39). In these assays, neutrophils from wild type or *munc13-4* KO mice were stimulated with fMLP or left untreated, and the distribution of endogenous p22^{phox}-containing granules in the exocytic active zone was analyzed by immunofluorescence microscopy using antibodies that specifically detect endogenous p22^{phox}. We found that the number of flavocytochrome b_{558}-expressing granules in unstimulated MUNC13-4 KO cells is similar to that present in the exocytic active zone of wild type cells (Fig. 1, *C* and *D*). However, although stimulated wild type neutrophils showed a marked increase in the number of p22^{phox}-positive vesicles in proximity to the plasma membrane, the number of vesicles at the exocytic active zone corrected by area unit did not significantly increase in MUNC13-4 KO cells after fMLP treatment (Fig. 1, *C* and *D*). Similar results were observed when the distribution of gp91^{phox}-positive vesicles was analyzed (data not shown). The deficient mobilization of flavocytochrome b_{558} in MUNC13-4 KO cells is most likely explained by a defect in the trafficking of gelatinase and specific granules, which contain more than 85% of the intracellular flavocytochrome b_{558}, toward the plasma
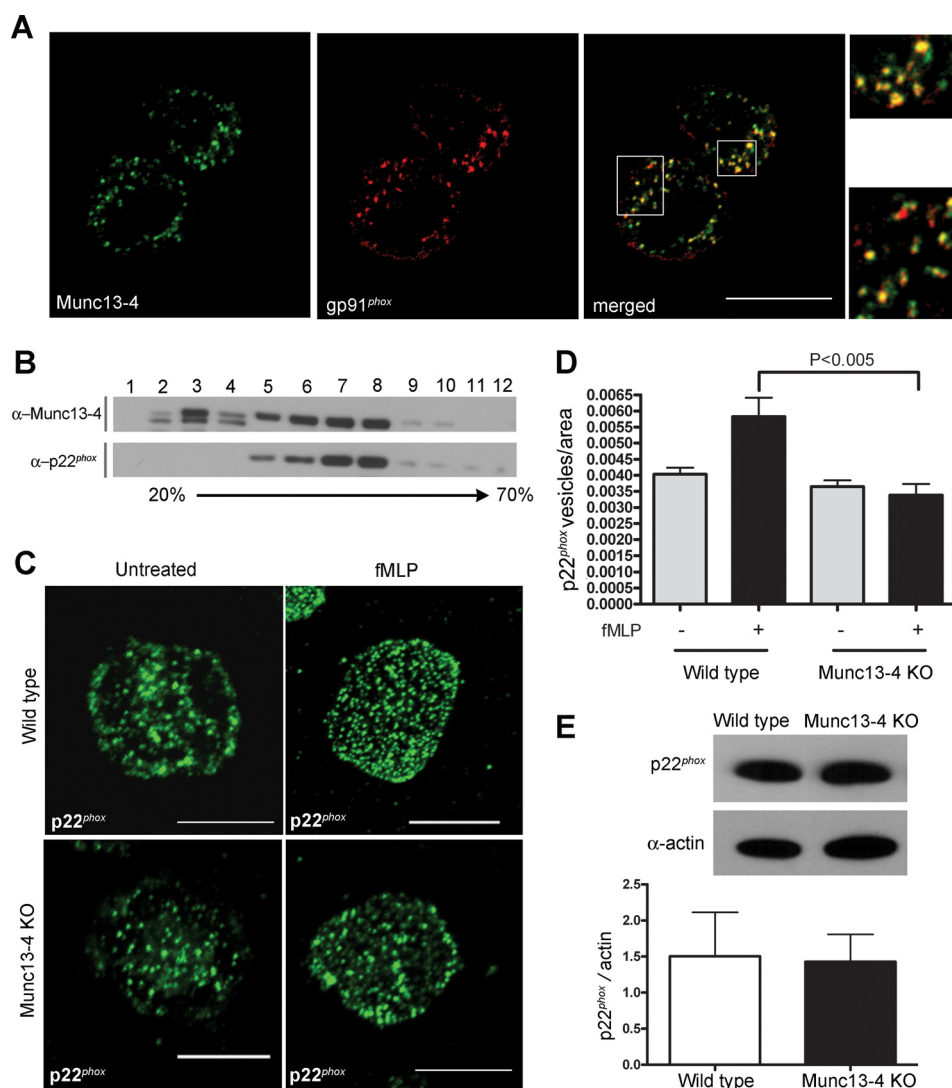
FIGURE 1. **Translocation of the p22^{phox}-expressing organelles at the exocytic active zone is impaired in MUNC13-4 KO neutrophils.** *A* and *B*, MUNC13-4 colocalizes and cofractionates with flavocytochrome b_{558}-expressing vesicles. *A*, neutrophils were fixed, and the subcellular localization of endogenous MUNC13-4 and gp91^{phox} at the exocytic active zone was analyzed by immunofluorescence using TIRF microscopy (*scale bars*, 10 μm). The colocalization of MUNC13-4 and gp91^{phox} in neutrophil granules is shown in the *inset*. *B*, neutrophils were lysed and fractionated using sucrose gradients, and endogenous proteins were analyzed by Western blot. *C*, decreased number of p22^{phox}-expressing organelles at the exocytic active zone in MUNC13-4 KO neutrophils. The distribution of p22^{phox}-expressing organelles at the exocytic active zone was analyzed by immunofluorescence using TIRF microscopy. Representative images of unstimulated or fMLP-stimulated wild type and MUNC13-4 KO neutrophils are shown (*scale bars*, 10 μm). *D*, quantitative analysis of the distribution of p22^{phox}-expressing vesicles at the exocytic active zone per area unit of MUNC13-4 KO and wild type neutrophils. A total of 80 wild type and 40 MUNC13-4 KO cells from three independent experiments were analyzed. Results are expressed as mean $\pm$ S.E. (*error bars*). *E*, the level of p22^{phox} expression in wild type and MUNC13-4 KO neutrophils was analyzed by Western blot and subsequently quantified. The data are representative of three independent experiments with similar results. Quantitative analysis represents the mean $\pm$ S.E. (*error bars*).

membrane. Defects in the translocation of flavocytochrome associated with the neutrophil organelle named the secretory vesicle (49) are unlikely because the mobilization of this subcellular organelle is not impaired in MUNC13-4 KO neutrophils (27). Next, to exclude the possibility that the lower number of p22^{phox}-positive granules visualized in the active zone of MUNC13-4 KO neutrophils was caused by decreased protein expression, we analyzed p22^{phox} expression by Western blot. No differences in the expression of p22^{phox} protein were found between wild type and MUNC13-4 KO neutrophils (Fig. 1*E*). Altogether, our data suggest that MUNC13-4 KO neutrophils may have a defective extracellular oxidative response due to deficient granule trafficking or impaired granule retention at the exocytic active zone.

The Integration of p22^{phox} into the Plasma Membrane Is Impaired in MUNC13-4 KO Neutrophils—MUNC13-4 has been proposed to regulate secretory organelle fusion (33, 50). To investigate a possible role for MUNC13-4 in the regulation of flavocytochrome b_{558} integration into the plasma membrane, we performed immunofluorescence and confocal microscopy analysis of wild type and MUNC13-4 KO neutrophils and labeled the plasma membrane with rhodamine-wheat germ agglutinin (WGA). In these assays, transversal images of fMLP-stimulated neutrophils were analyzed to determine putative differences in the insertion of p22^{phox}-containing membranes into the plasmalemma between wild type and MUNC13-4 KO neutrophils. Using this approach, we found that upon stimulation, p22^{phox}-positive granules translocate to
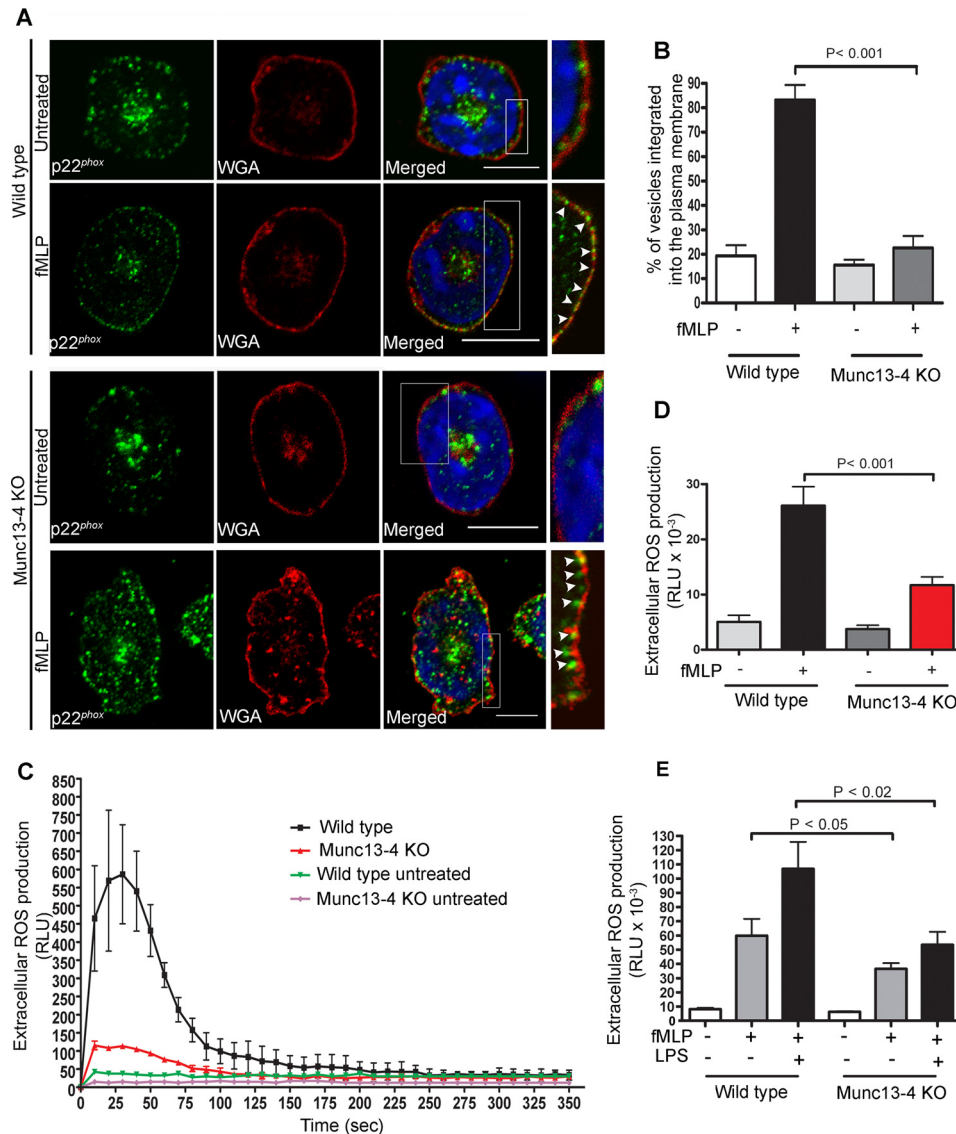
FIGURE 2. **MUNC13-4 KO neutrophils are characterized by an impaired integration of p22^{phox} into the plasma membrane and defective extracellular ROS production.** *A*, confocal microscopy analysis of the distribution of endogenous p22^{phox} in relationship to the plasma membrane. Wild type and MUNC13-4 KO neutrophils were left untreated or stimulated with 10 μM fMLP and fixed, and immunofluorescence analysis was performed using a polyclonal antibody specific for the detection of endogenous p22^{phox} and rhodamine-WGA to label the plasma membrane. The samples were analyzed by confocal microscopy, and representative *z*-sections for each condition are shown. *Inset*, the *arrowheads* point to p22^{phox}-positive granules, which are integrated into the plasma membrane in wild type cells but not in MUNC13-4 KO cells (*scale bars*, 10 μm). *B*, quantitative analysis showing the percentage of the p22^{phox}-containing vesicles in the exocytic active zone that are integrated into the plasma membrane. The results are representative of three independent experiments with similar results (mean ± S.E. (*error bars*)). *C*, ROS production was measured using bone marrow-derived neutrophils from MUNC13-4 KO and WT mice treated with the cell-impermeant probe isoluminol in the presence of horseradish peroxidase and stimulated with 10 μM fMLP. The representative graph shows the kinetics of extracellular ROS production, which is defective in MUNC13-4 KO cells (*red line* and *symbols*). *D* and *E*, quantitative determination of the total ROS produced during the time of analysis (calculated as the integral or area under the curve). Results are expressed as mean ± S.E. (*error bars*); statistical analysis was performed using a non-parametric Mann-Whitney test (*D*, $n = 8$; *E*, $n = 3$). *RLU*, relative light units.

and integrate into the plasma membrane in wild type cells, as visualized by the colocalization of the flavocytochrome-subunit p22^{phox} with WGA (Fig. 2*A*). In contrast, although p22^{phox}-expressing vesicles appeared to translocate to areas near the plasma membrane after stimulation in MUNC13-4 KO neutrophils, these organelles were unable to integrate into the plasmalemma as evidenced by their decreased colocalization with WGA (Fig. 2*A*). Quantification analysis shows that although 89.8 ± 14.1% of the p22^{phox} vesicles in the exocytic active zone colocalize with the marker WGA in fMLP-stimulated wild type cells, only 22.5 ± 14.0% of the p22^{phox} expressing-vesicles showed colocalization with the plasma membrane marker in

MUNC13-4 KO cells (Fig. 2*B*). Similar results were obtained when colocalization of p22^{phox}-positive granules was performed using the plasma membrane marker CD44 (data not shown). These data suggest that in addition to trafficking and docking (Ref. 30 and Fig. 1) MUNC13-4 regulates the fusion of flavocytochrome b_{558}-containing granules to the plasma membrane.

The Production of Extracellular NADPH Oxidase-dependent ROS Is Impaired in MUNC13-4 KO Neutrophils—To test whether the abnormal mobilization of flavocytochrome b_{558} was linked to a possible role of MUNC13-4 in the regulation of plasma membrane-associated ROS production, we next ana-

lyzed the generation of extracellular ROS in MUNC13-4 KO neutrophils. To analyze the contribution of the NADPH oxidase to extracellular ROS generation in real time, we used the cell-impermeant, ROS-dependent, chemiluminescent probe isoluminol in the presence of horseradish peroxidase as described (22, 51). Under these experimental conditions, isoluminol-mediated chemiluminescence is dependent on NADPH oxidase-derived ROS but independent of MPO. Neutrophils were stimulated with the chemotactic peptide fMLP, which is a well known inducer of extracellular superoxide anion in these cells (52). Here, we show that MUNC13-4 KO neutrophils have a marked impairment in NADPH oxidase-dependent extracellular oxidative response (Fig. 2C). The differences in the oxidative responses of MUNC13-4-deficient and wild type neutrophils were statistically significant (Fig. 2D), suggesting that MUNC13-4-dependent mechanisms are necessary to assemble the NADPH oxidase at the plasma membrane in neutrophils. MUNC13-4 has previously been implicated in priming of exocytosis, the mechanism that sensitizes neutrophils to amplify their response to a second stimulus (30). Then, to evaluate whether MUNC13-4 is involved in priming of the oxidative response, neutrophils were incubated with LPS before fMLP stimulation, an approach that better recapitulates the *in vivo* situation. In Fig. 2E, we show that the response of LPS-primed MUNC13-4 KO neutrophils to fMLP was significantly impaired. However, LPS pretreatment modestly increased the oxidative response in MUNC13-4 KO cells. This is most likely explained by the non-exocytic priming mechanisms of LPS including LPS-induced p47^{phox} phosphorylation (53).

To rule out the possibility that abnormal distribution of the flavocytochrome b_{558} could cause the impaired oxidative response in MUNC13-4 KO cells, we next analyzed the subcellular localization of endogenous flavocytochrome b_{558} in relationship to the distribution of several organelle/granule markers in MUNC13-4 KO neutrophils by confocal microscopy. We found normal distribution of p22^{phox} in MUNC13-4 KO cells that fully colocalizes with gp91^{phox} (supplemental Fig. S2, A–D) and partially colocalizes with the secretory vesicle marker CD35 (supplemental Fig. S2, E–H) in both unstimulated and stimulated MUNC13-4 KO neutrophils. As expected, p22^{phox} did not colocalize with MPO-containing granules in unstimulated MUNC13-4-KO or wild type neutrophils (supplemental Fig. S2, I–L). Furthermore, no differences were identified between MUNC13-4 KO and wild type cells in the distribution of p22^{phox} in relationship to the early endosome marker EEA1 (supplemental Figs. S2, M–P) or the secretory vesicle marker vesicle-associated membrane protein (not shown).

Intracellular ROS Production Is Defective in MUNC13-4 KO Neutrophils—In neutrophils, intraphagosomal ROS production facilitates the killing of internalized bacteria (20, 54). To evaluate whether MUNC13-4 regulates intraphagosomal ROS formation in response to physiological stimulation, we analyzed the oxidative response of MUNC13-4 KO neutrophils to the human pathogenic bacterium *P. aeruginosa*. In these experiments, we incubated wild type and MUNC13-4 KO neutrophils with live *P. aeruginosa* and analyzed ROS production using cell-permeant luminol. Under these experimental conditions, luminol-mediated chemiluminescence is dependent on both

NADPH oxidase and MPO-derived by-products. Here, we show that intracellular ROS is dramatically impaired in MUNC13-4-deficient neutrophils infected with *P. aeruginosa* (Fig. 3, A and B). No significant differences were observed in the maximal oxidative response time (peak) between MUNC13-4 KO and wild type neutrophils (3.50 ± 0.29 *versus* 4.63 ± 0.89 min, wild type *versus* MUNC13-4 KO, respectively; mean ± S.E., n = 6). Importantly, both the oxidative response to *P. aeruginosa* of wild type cells and the residual response of MUNC13-4 KO neutrophils to the bacteria were abolished when the cells were treated with the phagocytosis inhibitor cytochalasin D (Fig. 3, A and B). Furthermore, neutrophils incubated with cell-impermeant isoluminol showed a weak or no oxidative response to *P. aeruginosa* (Fig. 3C), indicating that *P. aeruginosa* triggers almost exclusively intracellular ROS production and suggesting that MUNC13-4 might regulate phagosomal assembly of the oxidase, phagocytosis maturation, or particle internalization.

MUNC13-4 Regulates Phagosome Maturation in Neutrophils—To determine whether defective intracellular ROS production could be due to a possible role of MUNC13-4 in uptake of bacteria, we next quantified fluorescently labeled live *P. aeruginosa* internalization by wild type and MUNC13-4 KO neutrophils by confocal microscopy. In these experiments, the cells were extensively washed, and the fluorescence of the few remaining non-internalized bacteria was quenched with trypan blue. Internalized bacteria were quantified in *z*-stacks covering the whole cell using confocal microscopy (Fig. 4). Our quantitative analyses show that MUNC13-4 KO neutrophils are able to internalize bacteria as efficiently as wild type cells (Fig. 4). In this way, neither the number of neutrophils with internalized bacteria (Fig. 4, A and B) nor the number of phagosomes per cell (Fig. 4, C and D) was different between wild type and MUNC13-4-deficient cells, suggesting that internalization of bacteria is a MUNC13-4-independent process.

Next, we evaluated whether the impaired intraphagosomal oxidative response observed in MUNC13-4 KO neutrophils was caused by a putative role of this protein in the trafficking and/or tethering of p22^{phox}-positive vesicles to the phagosome upon bacterial internalization. To this end, we performed phagocytosis analysis of wild type and MUNC13-4 KO neutrophils treated with rhodamine-labeled, opsonized, live *P. aeruginosa* and determined the subcellular localization of endogenous p22^{phox} by confocal microscopy using antibodies that recognize the endogenous protein. In these assays, phagosomal localization of p22^{phox} was analyzed 15 min after the initiation of the synchronized phagocytosis assay. In Fig. 5A, we show that p22^{phox} translocates to the phagosome and integrates with the phagosomal membrane in both neutrophils lacking MUNC13-4 and wild type cells. Quantitative analysis revealed that the number of p22^{phox}-positive phagosomes in MUNC13-4 KO neutrophils was not significantly different from that observed in wild type neutrophils (Fig. 5B).

Phagocytic vacuoles acquire degradative and microbicidal properties through the sequential fusion with intracellular organelles. In neutrophils, phagosome maturation is characterized by the fusion of the phagosome with several vesicles including azurophilic granules and multivesicular bodies (2,
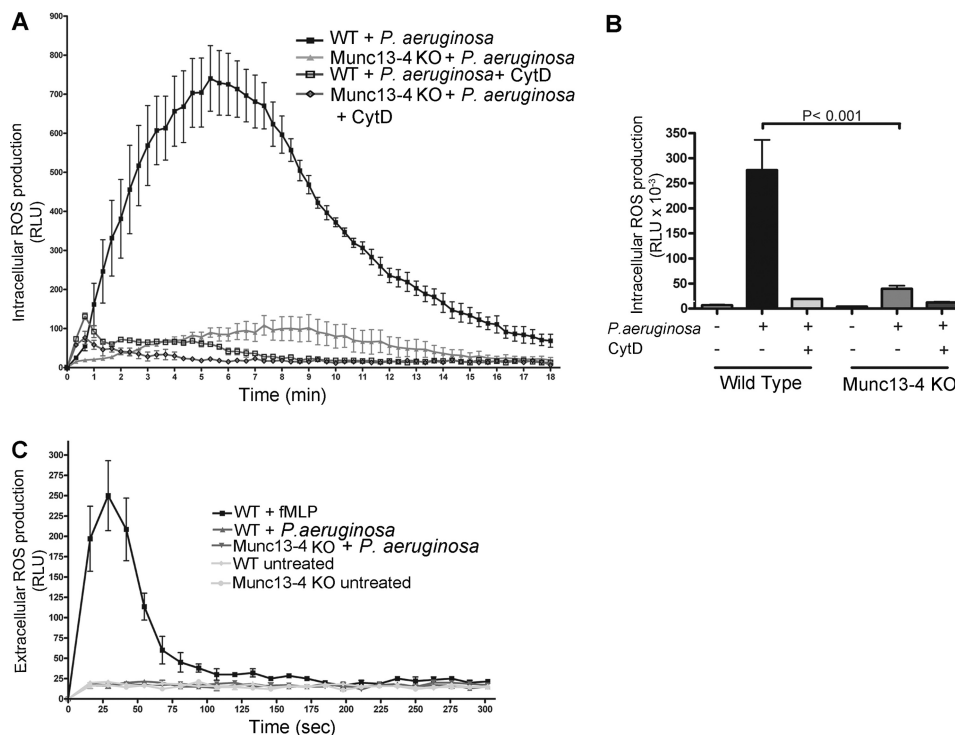
FIGURE 3. **MUNC13-4 KO neutrophils have impaired intracellular ROS production.** *A*, neutrophils from MUNC13-4 KO and wild type mice were incubated with serum-opsonized *P. aeruginosa* at a ratio of 10:1 (bacteria/neutrophil), and intracellular ROS production was analyzed by the luminol-dependent chemiluminescence reaction. Reactions were started by the addition of bacteria to a prewarmed (37 °C) neutrophil suspension, and chemiluminescence was continuously monitored from this time point. Where indicated, the inhibitor of phagocytosis cytochalasin D (*CytD*; 10 μg/ml) was used as control. *B*, quantitative determination of the total ROS produced during the time of analysis (calculated as the integral or area under the curve). Results are expressed as mean ± S.E. (*error bars*) from six independent experiments. *C*, undetectable extracellular ROS production induced by *P. aeruginosa*. The extracellular oxidative response was measured using cell-impermeant isoluminol in the presence of horseradish peroxidase. Different from fMLP, live *P. aeruginosa* was unable to induce an extracellular oxidative response under these assay conditions. *RLU*, relative light units.

55). The observation that intraphagosomal ROS production was impaired in MUNC13-4 KO neutrophils but translocation of flavocytochrome b_{558} to the phagosomal membrane was not affected suggested a possible role of MUNC13-4 in the trafficking of MPO-positive granules to the phagosome. Importantly, we have reported previously that MUNC13-4 localizes at a subpopulation of azurophilic granules (27) and that MUNC13-4 regulates azurophilic granule trafficking in neutrophils (30), but a possible role for MUNC13-4 in trafficking during phagocytosis has not been explored. To investigate whether MUNC13-4 plays a role in regulating the fusion of phagosomes with azurophilic granules, we analyzed the subcellular distribution of MPO-positive organelles during phagocytosis by quantitative immunofluorescence confocal microscopy. To this end, we exposed wild type and MUNC13-4 KO neutrophils to rhodamine-labeled, opsonized *P. aeruginosa* for 45 min and stained with MPO antibodies. We found that whereas 73.3 ± 3.2% of phagosomes in wild type neutrophils were positive for MPO staining, MUNC13-4-deficient cells showed MPO-positive granules in association with only 28.5 ± 4.4% of their phagosomes (Fig. 5, *C* and *D*). Furthermore, MPO-positive staining in MUNC13-4 KO neutrophils showed a punctate staining close to the phagosome rather than integration with the phagosomal membrane, representing non-fused azurophilic granules (Fig. 5*C*, *arrowheads*), suggesting that MUNC13-4 is necessary for azurophilic granule fusion with the phagosome.

To evaluate whether MUNC13-4 function in phagosomal maturation is exclusively associated with azurophilic granule fusion or it is extended to other intracellular organelles, we next evaluated whether MUNC13-4 regulates the mechanism of MVB fusion with the phagosome. MVBs bear the integral membrane protein LAMP1 (6), which has been proposed to directly regulate phagosomal maturation (24). Furthermore, MVB fusion with phagosomes has been shown to be important to complete the maturation process (56). Here, we show that MVB recruitment to the phagosomes is impaired in MUNC13-4 KO cells (Fig. 5*E*) with 18.8 ± 5.6% of their phagosomes containing LAMP1. This is significantly different from that observed in wild type neutrophils in which 80.9 ± 5.6% of the phagosomes integrated LAMP1 to the phagosomal membrane 45 min after the initiation of the synchronized assay (Fig. 5*F*). Altogether, these data suggest that MUNC13-4 is important for azurophilic granule and MVB delivery to the phagosome and fusion with the phagosomal membrane. Consequently, several steps required for phagosome maturation are impaired in the absence of MUNC13-4.

Intracellular ROS Production and Phagosomal Maturation Are Normal in RAB27A KO Neutrophils—RAB27A and its effector MUNC13-4 are master regulators of exocytosis in neutrophils (26, 27, 29, 30). Furthermore, similar to that shown in this work for MUNC13-4, RAB27A also plays an important role in the regulation of the neutrophil extracellular oxidative response (28). However, we and others have shown previously that MUNC13-4 is able to regulate some cellular functions in a RAB27A-independent manner (30, 57), and previous studies from our laboratory indicate that RAB27A does not integrate
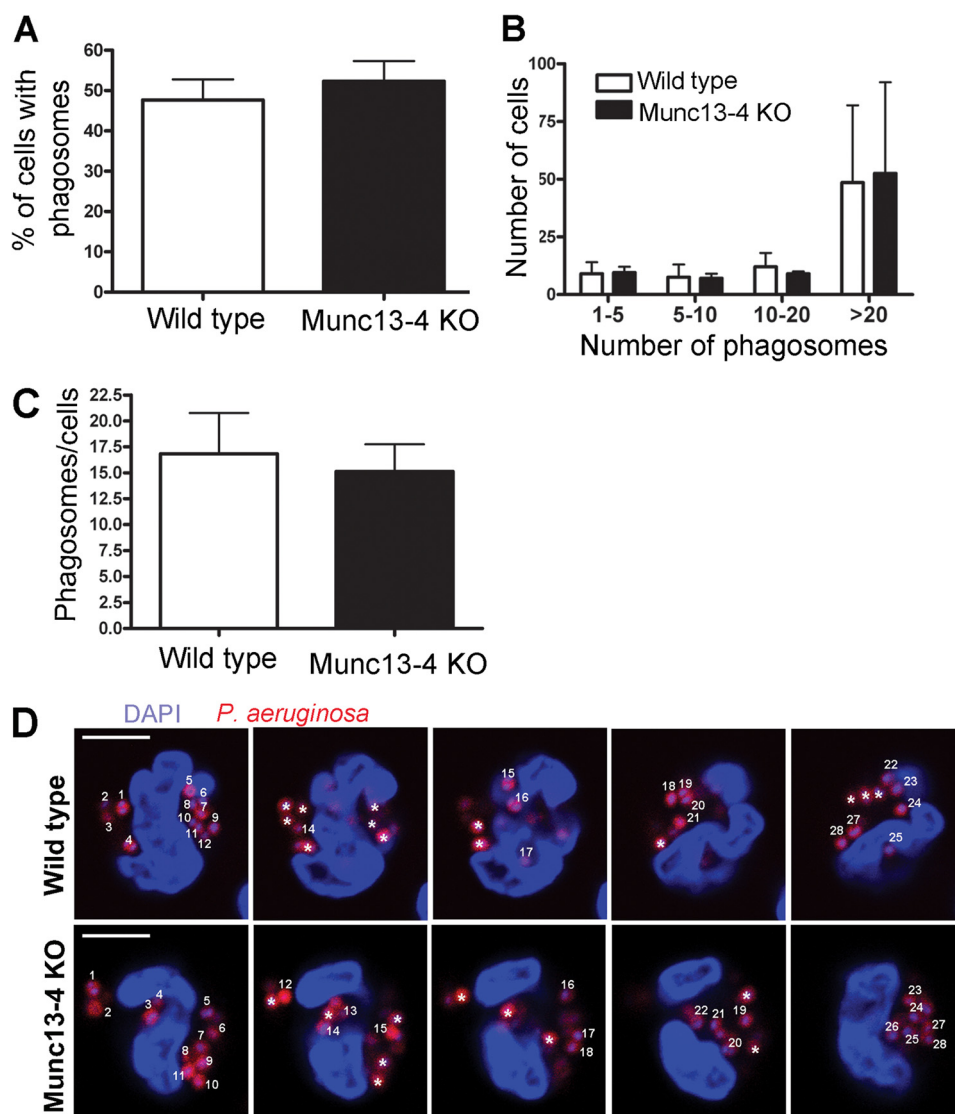
FIGURE 4. **MUNC13-4 KO neutrophils have normal phagocytic activity.** Confocal microscopy analysis was performed to quantify live *P. aeruginosa* internalization in wild type and MUNC13-4 KO neutrophils. Cells were incubated with opsonized, tetramethylrhodamine-conjugated *P. aeruginosa* for 45 min at 37 °C. Fluorescent extracellular bacteria were quenched with trypan blue, and internalized bacteria were counted manually from up to 10 section fields for each sample. No significant differences were observed in the percentage of cells containing phagosomes (*A*) between wild type and MUNC13-4 KO cells. *B*, the distribution of the cell populations containing increasing numbers of phagosomes was also similar in wild type and MUNC13-4 KO cells. *C*, no significant differences were observed in the average number of phagosomes/cell between MUNC13-4 KO and wild type neutrophils. The results are mean ± S.E. (*error bars*) from three independent experiments. *D*, representative image of confocal sections used to count the number of bacteria present in each cell population. * indicates bacteria already counted in the previous *z*-section. The thickness of each stack is 0.5 μm (*scale bars*, 10 μm). Individual intracellular bacteria are indicated with *numbers*.

with the phagosomal membrane in neutrophils (26, 28). Here, we investigated a possible role of RAB27A in the phagosomal oxidative response and in the regulation of phagosomal maturation induced by *P. aeruginosa*. First, to analyze the ability of RAB27A to mediate phagosomal ROS production, wild type and RAB27A KO neutrophils were incubated in the presence of *P. aeruginosa*, and intraphagosomal ROS was determined using the luminol-dependent chemiluminescence assay. Different from that observed for MUNC13-4 KO cells, which showed a marked deficiency in their oxidative response (Fig. 3), we found that the oxidative response triggered by phagocytosis of opsonized, live bacteria was not affected in RAB27A KO neutrophils (Fig. 6A). This is in agreement with previous studies from our laboratory showing that RAB27A KO neutrophils

have a normal intraphagosomal oxidative response to heat-killed *Listeria monocytogenes* (28). Moreover, confocal microscopy analysis revealed that, different from that observed in MUNC13-4 KO neutrophils, MPO and LAMP1 recruitment to the phagosomes was not affected in RAB27A KO cells (Fig. 6B).

MUNC13-4 KO Neutrophils Have Impaired Bactericidal Activity—The ultimate function of bacterial internalization and phagosome maturation in neutrophils is to promote bacterial killing. Because MUNC13-4-deficient neutrophils showed defective phagosome maturation (Fig. 5), we next evaluated whether MUNC13-4 KO neutrophils have impaired ability to kill bacteria. To this end, we first performed a bactericidal assay based on the lysis of neutrophils and quantification of both internalized-then-released and extracellular live bacteria. In
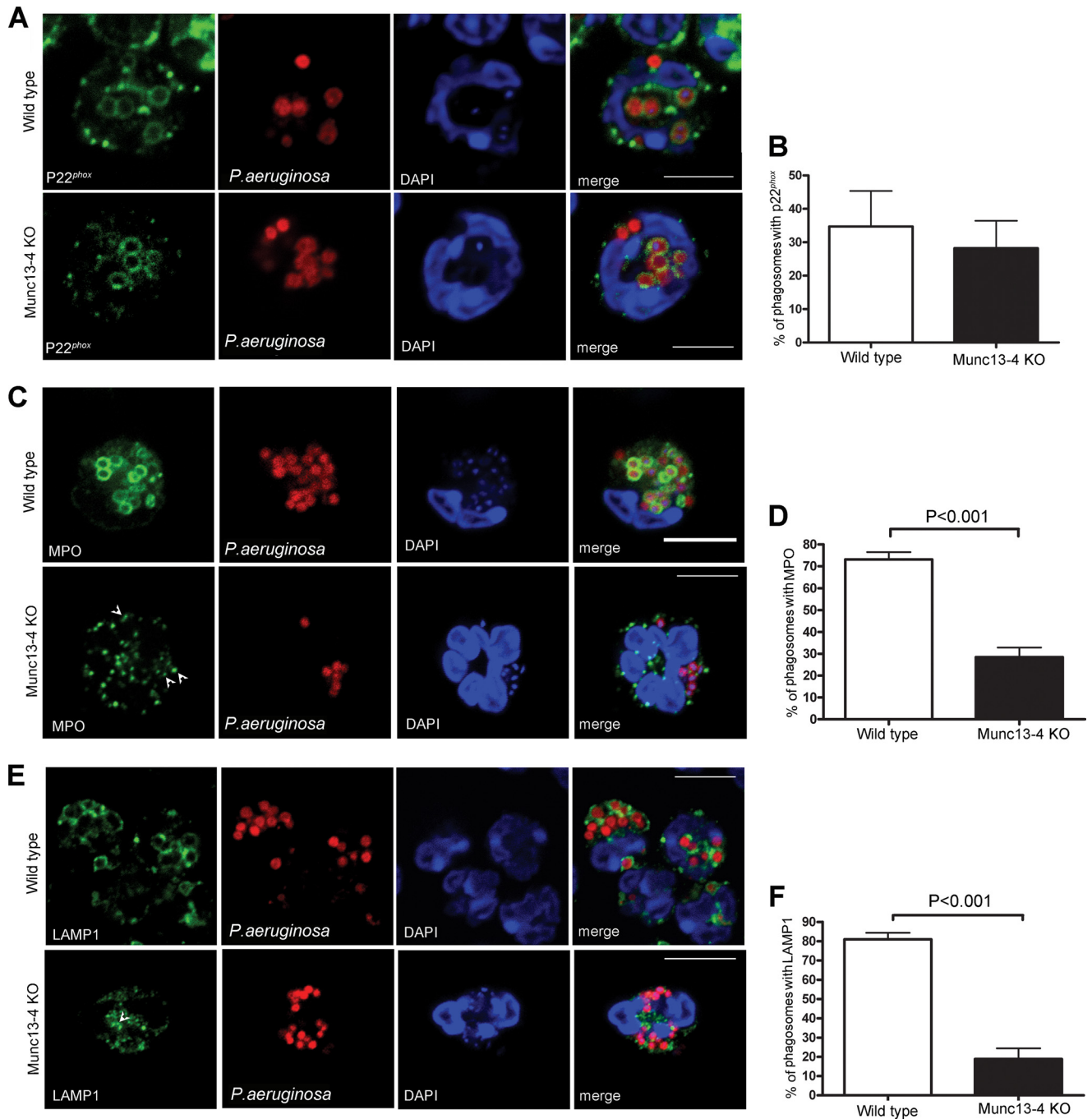
FIGURE 5. **Phagosomal maturation is impaired in MUNC13-4 KO neutrophils.** Wild type and MUNC13-4 KO neutrophils were incubated with opsonized, tetramethylrhodamine-conjugated *P. aeruginosa* at 4 °C, and synchronized phagocytosis was started by incubation of the neutrophil/bacteria mixture at 37 °C for 15 (*A* and *B*) or 45 min (*C–F*). *A*, the subcellular localization of endogenous p22^{phox} was analyzed by immunofluorescence. *B*, the percentage of p22^{phox}-positive phagosomes was calculated by analyzing 187 and 282 phagosomes from wild type and MUNC13-4 KO cells, respectively. *C*, the subcellular localization of endogenous MPO was analyzed by immunofluorescence. *D*, the percentage of the phagosomes that were positive for MPO staining was calculated by analyzing 880 and 657 phagosomes from wild type and MUNC13-4 KO cells, respectively. *E*, analysis of endogenous LAMP1 localization was performed as described above. *F*, the percentage of LAMP1-positive phagosomes was determined after counting a total of 759 and 633 phagosomes in wild type and MUNC13-4 KO cells, respectively. Results are expressed as mean ± S.E. (*error bars*) from three independent experiments. *Scale bars*, 10 μm.

this assay, wild type and MUNC13-4 KO neutrophils were incubated with opsonized *P. aeruginosa* for 3 h and subsequently used in killing assays. The viability of the released bacteria was then determined using the formazan dye XTT, which acts as an artificial electron acceptor of the electron transport chain (58), used previously to detect microbial respiration events of *P. aeruginosa* (59) and quantified by spectrophotom-

etry as described previously (43). This analysis revealed that MUNC13-4 KO neutrophils have a significantly impaired bactericidal activity. In this way, only ~40% of the bacteria were killed by MUNC13-4 KO cells, whereas ~60% of the bacteria were killed by wild type neutrophils under the exact experimental conditions (Fig. 7*A*). As mentioned above, no differences were found in the number of internalized bacteria between wild
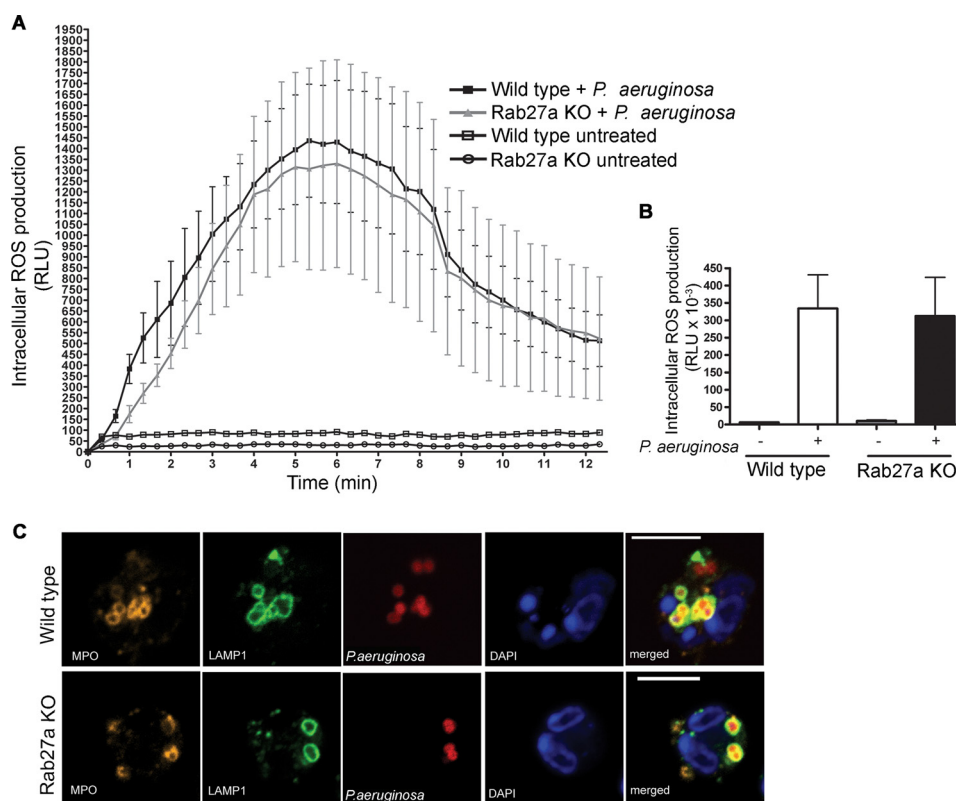
FIGURE 6. **RAB27A is not required for bacterium-induced intracellular ROS production or phagosomal maturation.** *A* and *B*, neutrophils from RAB27A-deficient and WT mice were incubated with opsonized *P. aeruginosa*, and the luminol-dependent chemiluminescence reaction was monitored for the indicated time. The kinetics are representative of three independent experiments. *B*, quantitative analysis of *P. aeruginosa*-induced ROS production. The results are expressed as mean ± S.E. (*error bars*). *C*, confocal microscopy analysis of the distribution of endogenous MPO and LAMP1 in wild type and RAB27A-deficient cells after phagocytosis of serum-opsonized, tetramethylrhodamine-conjugated *P. aeruginosa* for 45′ at 37 °C. *Scale bars*, 10 μm. *RLU*, relative light units.

type and MUNC13-4 KO cells (Fig. 4), so differences observed in killing assays are most likely explained by the intraphagosomal bactericidal defects of MUNC13-4 KO neutrophils. Next, we tested the ability of MUNC13-4 KO neutrophils to kill extracellular bacteria using the same spectrophotometric approach used to measure the survival of non-internalized bacteria. Interestingly, differences in extracellular bacterial killing between wild type and MUNC13-4-deficient cells were only observed when neutrophils were treated with DNase I after the 3-h incubation time, assay conditions that favor the release of trapped bacteria from NETs (Fig. 7*B*). This suggested that a relatively small but significant number of bacteria were trapped in NETs but not killed by MUNC13-4 KO cells. Because MUNC13-4 KO neutrophils have deficient exocytosis (27, 30) and impaired extracellular ROS production (Fig. 2), our results suggested, in principle, that defects in either or both of these mechanisms could be responsible for the deficient extracellular killing observed in MUNC13-4 KO cells. To determine whether NADPH oxidase-derived ROS was necessary to kill *P. aeruginosa* by neutrophils, we next used gp91^{phox} KO neutrophils in killing assays. Our data, presented in Fig. 7*C*, show that the oxidase is dispensable for neutrophil-mediated killing of *P. aeruginosa*. This is in agreement with previous reports showing that neutrophils from CGD patients efficiently kill *P. aeruginosa* but not *Pseudomonas cepacia* (60). Altogether, our data suggest that impaired phagosomal maturation and perhaps deficient exocytosis (30) are responsible for the defective killing of *P. aeruginosa* in MUNC13-4 KO neutrophils.

MUNC13-4 KO Neutrophils Show Increased NET Production Compared with Wild Type Neutrophils—NETs are known to contribute to the elimination of pathogenic bacteria, and NET formation is deficient in certain immunodeficiencies (3, 41). The finding that MUNC13-4-deficient cells showed impaired killing of non-internalized, putative NET-trapped bacteria prompted us to investigate whether MUNC13-4 KO cells produce normal neutrophil extracellular traps. To analyze whether MUNC13-4 KO neutrophils were able to produce NETs in response to live bacteria, neutrophils were incubated with live *P. aeruginosa* for 3 h, samples were fixed, DNA was stained with DAPI, and NET production was subsequently analyzed by quantitative confocal microscopy. Our results revealed that NET production was 2-fold higher in MUNC13-4 KO neutrophils than in wild type cells (Fig. 8*A*). Thus, although ~30% of MUNC13-4 KO cells produced NETs under our assay conditions, only ~15% of wild type cells were able to induce extracellular trap formation in wild type cells (Fig. 8*B*). We observed similar results when NETs were evaluated using DNA dyes (Fig. 8*C*). Because NET function is believed to be mediated by neutrophil granular proteins that localize on the extracellular DNA fibers (4) and because the release of granule cargoes to the extracellular milieu is defective in MUNC13-4 KO neutrophils (30), we next determined whether NETs from MUNC13-4 KO neutrophils contain neutrophil granular proteins. Using immunofluorescence analysis of endogenous proteins, we observed that NETs from MUNC13-4 KO neutrophils are decorated with puncta that were positive for MPO (Fig. 8*D*), suggesting
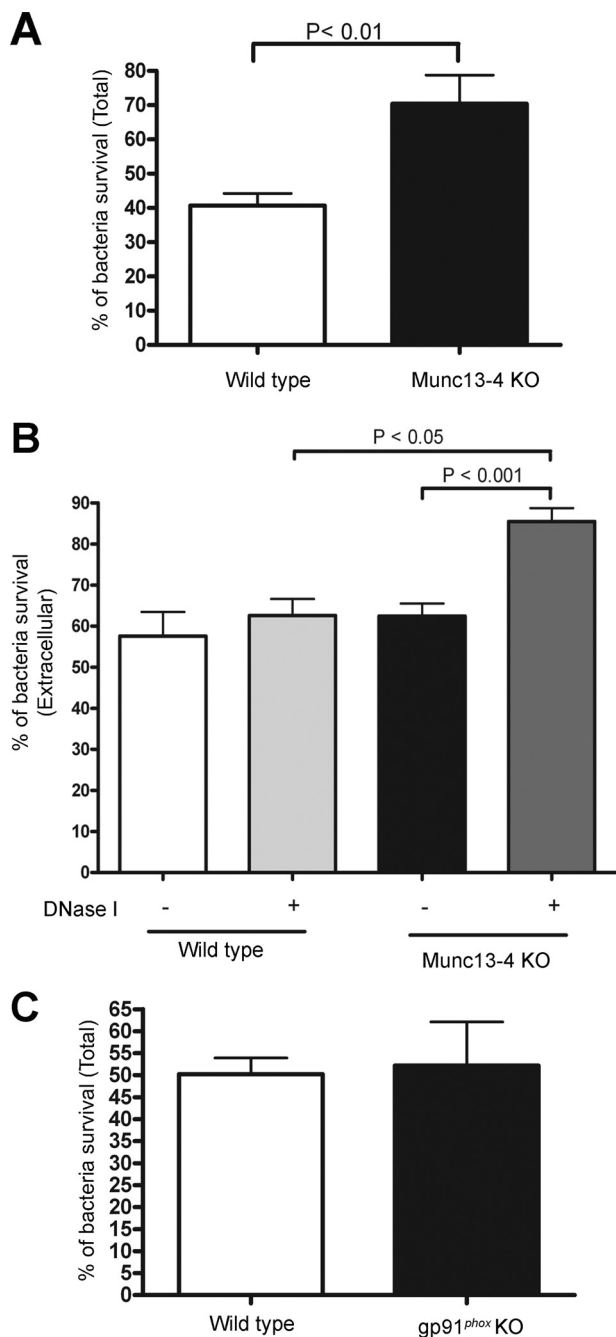
A

B

C

FIGURE 7. **MUNC13-4 KO neutrophils have impaired bacterial killing.** *A*, the ability of wild type and MUNC13-4 KO neutrophils to kill opsonized *P. aeruginosa* was analyzed by incubating freshly isolated neutrophils or heat-killed neutrophils (negative control) in the presence of opsonized *P. aeruginosa* for 3 h at 37 °C followed by release of internalized live bacteria by alkaline lysis of neutrophils at pH 11 and subsequent quantification of live bacteria by the XTT reaction as described under "Experimental Procedures." *B*, the ability of WT and MUNC13-4 KO neutrophils to kill extracellular bacteria was measured as described above except that alkaline lysis was omitted, and therefore, only extracellular bacteria were quantified. Where indicated, the cells were treated with DNase I to destroy neutrophil extracellular traps after the 3-h incubation period. The results are expressed as mean ± S.E. (*error bars*) (*n* = 6). Quantitative analysis was performed using a non-parametric Mann-Whitney test. *C*, *P. aeruginosa* killing by gp91^{phox} KO neutrophils was analyzed as described in *A*. The results are expressed as mean ± S.D. (*error bars*) (*n* = 2).

that MUNC13-4 KO neutrophils are able to produce potentially functional NETs. Altogether, our killing and NET generation data suggest that a complementary mechanism (*e.g.* exo-

cytosis (27)) may be necessary for MUNC13-4 KO neutrophils to efficiently kill *P. aeruginosa* that have been trapped by NET-forming cells.

DISCUSSION

MUNC13-4 regulates exocytosis in neutrophils (27, 29, 30), cytotoxic T lymphocytes (61), natural killer cells (62), and platelets (50, 63), and its deficiency is associated with the severe and often fatal immunodeficiency FHL3 in humans. In this work, we characterized novel, important roles for MUNC13-4 in the regulation of the neutrophil oxidative response, phagosomal maturation, and bacterial killing. Thus, we demonstrate that MUNC13-4 regulates the production of both extracellular and intracellular ROS through mechanisms that involve the control of vesicular trafficking and granular fusion. We also show that MUNC13-4 regulates the fusion of azurophilic granules and multivesicular bodies with the phagosome and that MUNC13-4 is necessary for the efficient killing of intraphagosomal pathogens. Based on experiments using gp91^{phox}-deficient neutrophils and previous data from CGD patients (60), it is possible that the defects in ROS production may not be causative of *P. aeruginosa* survival in MUNC13-4 KO neutrophils. However, it is likely that the impairment in ROS production would render MUNC13-4-deficient patients susceptible to infections by other catalase-positive pathogens. Altogether, our findings help to elucidate the molecular mechanisms of neutrophil-mediated killing and have direct implications on the understanding of the development of bacterial infections associated with FHL3.

The activation of the NADPH oxidase in response to soluble stimuli involves the translocation of the membrane-associated subunit of the oxidase, the flavocytochrome b_{558}, from the membrane of intracellular granules to the plasmalemma. In this work, we characterized MUNC13-4 as an essential regulatory component of this process. In particular, we show that MUNC13-4 controls discrete steps during the trafficking of flavocytochrome b_{558}-containing granules to the plasma membrane. MUNC13-4 has been proposed to regulate vesicular priming, tethering (30, 47), and fusion (33, 50), but simultaneous regulation of these mechanisms by MUNC13-4 in a single cellular system has not been shown. In this study, TIRF microscopy analysis of the distribution of p22^{phox}-expressing granules indicated that MUNC13-4-deficient neutrophils have a decreased number of granules at the plasma membrane (Fig. 1). In principle, this may suggest that MUNC13-4 regulates either granule trafficking toward the plasma membrane or granule tethering and retention at the plasma membrane. This is in agreement with the previous role described for MUNC13-4 in tethering of lytic granules in secretory lysosomes (47). In an independent approach, we show that a subpopulation of p22^{phox}-positive granules can be tethered at the plasma membrane but do not integrate with the plasmalemma upon stimulation (Fig. 2). This is also in agreement with a previous study showing that lytic granules are able to dock but not fuse at the immunological synapse in cytotoxic T lymphocytes lacking MUNC13-4 (33) and with a recent *in vitro* study showing that MUNC13-4 directly binds SNAREs and controls vesicular fusion (50). Our data suggest that rather than regulating a single
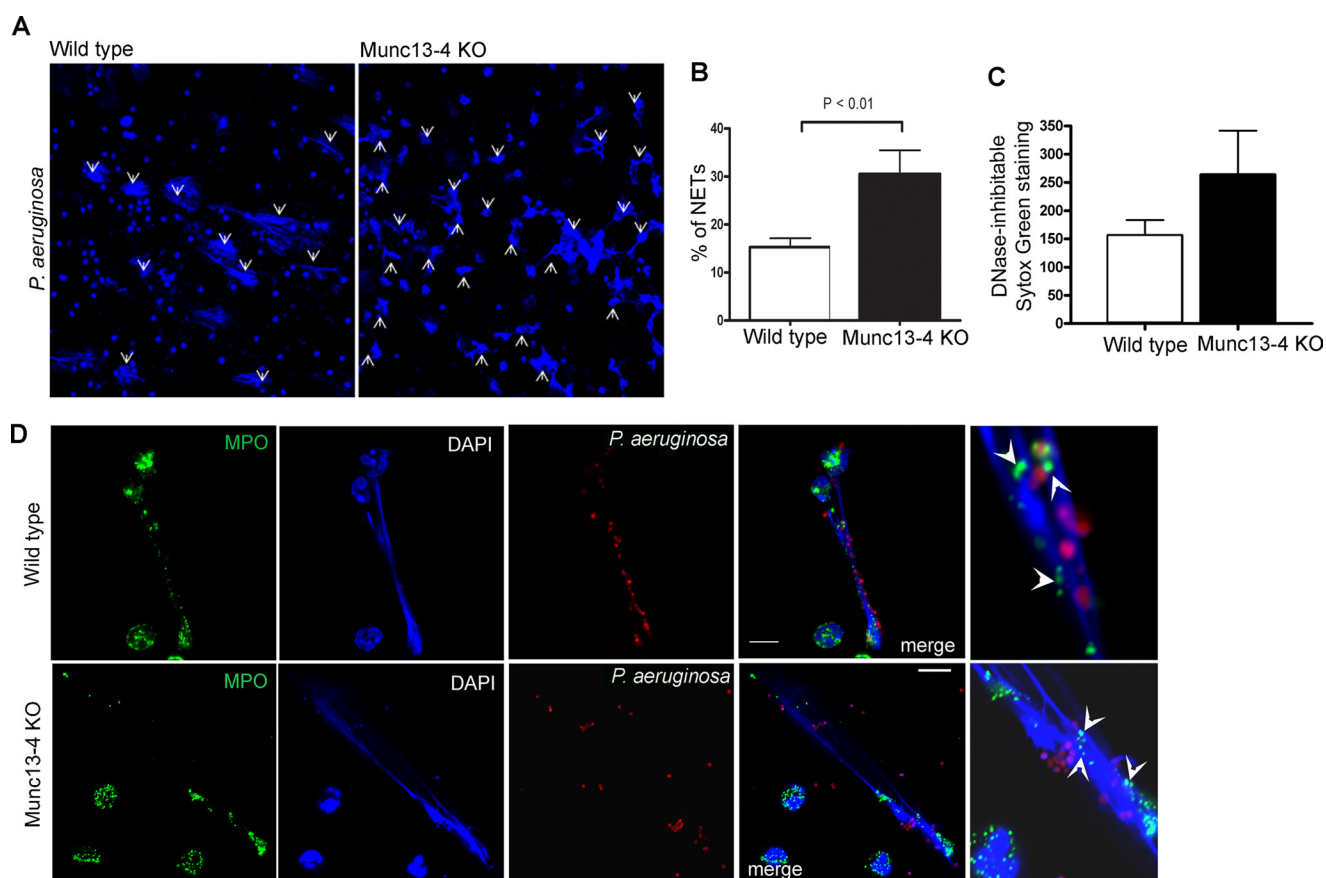
FIGURE 8. **NET production is increased in MUNC13-4 KO neutrophils.** *A*, wild type and MUNC13-4 KO neutrophils were incubated for 3 h in the presence of *P. aeruginosa*, stained with DAPI, and analyzed by confocal microscopy. Representative images of NETs produced by neutrophils are shown. *B*, NETs were counted from 10 independent fields for each sample using ImageJ software, and the percentages of NET-producing cells were calculated. Results are mean ± S.E. (*error bars*) from three independent experiments. Similar results were obtained using the cell-impermeant DNA dye SYTOX Green (*C*). *D*, confocal micros-copy analysis of neutrophil NETs after incubation with opsonized, tetramethylrhodamine-conjugated *P. aeruginosa* (*red*) shows a similar distribution of MPO (*green*; *arrowheads*) along NETs in wild type and MUNC13-4 KO cells. *Scale bars*, 10 μm.

step during granule trafficking MUNC13-4 regulates both teth-ering and fusion of p22^{phox}-expressing granules with the plas-malemma in neutrophils.

Phagocytosis in neutrophils is a process of fundamental importance for the innate immune response (2, 64), but the mechanisms underlying trafficking and fusion of neutrophil granules with the phagosome are not well understood. Our data show, for the first time, that MUNC13-4 regulates granule fusion with the phagosome and contributes to the formation of mature phagosomes in neutrophils. In our studies, MUNC13-4 selectively controlled the delivery of azurophilic granule and MVB proteins to the phagosome, whereas the translocation of the flavocytochrome b_{558} was not significantly affected in cells lacking MUNC13-4 expression. It is possible that the flavocy-tochrome b_{558} incorporated into the phagosome in cells lacking MUNC13-4 is derived from the plasma membrane and incor-porated into the phagosomal membrane during particle invag-ination. Alternatively, it is possible that MUNC13-4 does not regulate the fusion of flavocytochrome b_{558}-expressing gelatin-ase and/or specific granules with the phagosome. This would suggest that the subpopulation of flavocytochrome b_{558}-posi-tive granules that also contains MUNC13-4 is involved in traf-ficking toward the plasma membrane and not in vesicular transport to the phagosome or that alternative mechanisms

facilitate the delivery of the flavocytochrome b_{558} to the phago-some in the absence of MUNC13-4. Our data also suggest that MUNC13-4 is important for the production of intraphago-somal oxidants because it is responsible for the delivery of myeloperoxidase, the enzyme that catalyzes the formation of oxidized halides, which in turn contribute to intraphagosomal bacterial killing, from azurophilic granules (54, 65). In addition to myeloperoxidase, azurophilic granules are also important for the delivery of toxic proteases (*e.g.* elastase and cathepsin G) and bactericidal peptides into the phagosome. Therefore, the role played by MUNC13-4 in the regulation of azurophilic granule fusion with the phagosome is highly significant. Also important, our studies indicate that MUNC13-4 controls the fusion of LAMP1-positive MVBs with the phagosome. This is significant because in the absence of LAMP1 phagosomes show defective phagosomal maturation and trafficking and are pre-disposed to develop maturation arrest despite the normal activ-ity of other important regulators of phagosomal maturation including Rab7 (24).

Phagosomal maturation was not defective in the absence of RAB27A expression as RAB27A-deficient neutrophils in con-trast to MUNC13-4 KO neutrophils are able to deliver azuro-philic and specific granule proteins to the phagosomal mem-brane in response to *P. aeruginosa*. Although MUNC13-4 is

considered a specific RAB27A effector, previous studies have reported other MUNC13-4 functions that proceed in the absence of RAB27A. These include the exocytosis of a readily releasable subpopulation of azurophilic granules in neutrophils (30), the recruitment of MUNC13-4 to lytic granules in response to the activation of certain cellular receptors (31), and the regulation of exocytosis in platelets (63). How MUNC13-4 regulates phagosomal maturation and which upstream mechanisms activate MUNC13-4 are still unclear. Phagocytosis can proceed in the absence of RAB27A, but whether RAB27A is not involved at all in this process or whether MUNC13-4 interacts with other Rab proteins, which compensate for the absence of RAB27A, is still obscure. A recent report has presented evidence that phagosomal maturation is regulated by a relatively large network of Rab GTPases and that the number and type of Rab proteins engaged depend on the type of microorganism phagocytosed (66). Some of the candidates, which include Rabs 20, 22b, 32, 34, 38, and 43, were proposed to regulate phagosomal maturation in macrophages (66). Thus, it is possible that granule trafficking toward the phagosome is facilitated by Rab proteins other than RAB27A that would facilitate MUNC13-4 function in the granule/phagosomal fusion process. Future studies are necessary to determine whether or not these Rab proteins regulate MUNC13-4 function or play a significant role in neutrophils. Another possibility is that MUNC13-4 regulates granular-phagosomal fusion through direct interaction with SNARE proteins. In this way, the MUNC13-4 C2A domain has been recently shown to specifically interact with several SNAREs including syntaxins 1, 2, 4, and 11 but not syntaxins 3, 5, and 6 (50). In addition, MUNC13-4 is able to bind to phospholipids through its C2 domains (29). This ability of MUNC13-4 to interact with multiple molecular targets through independent intramolecular domains suggests that vesicle-associated MUNC13-4 would be able to interact with phagosomal targets and build a bridge between organelles to facilitate docking and/or fusion in a RAB27A-independent manner. Finally, two MUNC13-4-interacting proteins, RAB27A and syntaxin 11, have been postulated to act as negative regulators of phagocytosis (67, 68). These observations together with the findings that MUNC13-4 KO but not RAB27A KO neutrophils have defective phagosomal maturation may suggest that these MUNC13-4-interacting proteins may inhibit phagocytosis by sequestering MUNC13-4.

The mechanisms used by neutrophils to kill bacteria rely on their capacity to generate reactive oxygen species and to deliver serine proteases and bactericidal peptides into the extracellular milieu and the phagosome. In this work, we show that MUNC13-4 controls phagosomal maturation and is necessary to mediate efficient intracellular killing. Furthermore, extracellular killing defects in MUNC13-4 KO cells were also observed under experimental conditions that favor the release of NET-trapped bacteria. However, MUNC13-4 KO neutrophils produce a significantly higher number of NETs than wild type neutrophils when stimulated with live bacteria, and NETs in MUNC13-4 KO cells were decorated with the bactericidal protein myeloperoxidase, which is an important component for efficient NET formation and NET-dependent killing (4, 41, 69). Thus, it is possible that NET-mediated killing requires either

the release of secretory proteins or ROS production, two processes that are impaired in MUNC13-4 KO neutrophils (Refs. 29 and 30 and this work). For example, a steady supply of H_2O_2 is necessary to mediate the NET-associated MPO-dependent oxidative activity. Also, MUNC13-4 KO cells may be unable to generate an appropriate microenvironment to facilitate the catalytic activity of NET-associated proteases. A different scenario would take place in CGD neutrophil-mediated killing because neutrophils from CGD patients are unable to produce ROS and are completely devoid of NETs (41). These mechanisms are currently under investigation in our laboratory.

MUNC13-4 is ubiquitously expressed in hematopoietic cells, and its deficiency is associated with a severe immunodeficiency in humans characterized by the development of an accelerated phase usually referred to as hemophagocytic syndrome (33). This phenotype is generally associated with the impairment of natural killer cells and cytotoxic T lymphocytes to kill infected cells. However, recent evidence suggests that neutrophils may be involved in the development of hemophagocytic lymphohistiocytic syndrome (70), and patients with FHL3 have been found to suffer recurrent bacterial infections with granulomatous lung or liver disease in addition to well documented viral infections (71). These data together with our data presented here that neutrophils deficient in MUNC13-4 are characterized by impaired ROS production, phagocytosis maturation, and killing strongly support the view that neutrophil defects may contribute to the severe susceptibility to infections observed in FHL3 patients. In conclusion, our research shows that MUNC13-4 has previously unrecognized functions in intracellular granular trafficking, phagosomal maturation, and bacterial killing in neutrophils and highlights MUNC13-4 as a potential target for therapeutic intervention for the treatment of bacterial infections.

REFERENCES

1. Nathan, C. (2006) Neutrophils and immunity: challenges and opportunities. *Nat. Rev. Immunol.* **6,** 173–182
2. Lee, W. L., Harrison, R. E., and Grinstein, S. (2003) Phagocytosis by neutrophils. *Microbes. Infect.* **5,** 1299–1306
3. Brinkmann, V., Reichard, U., Goosmann, C., Fauler, B., Uhlemann, Y., Weiss, D. S., Weinrauch, Y., and Zychlinsky, A. (2004) Neutrophil extracellular traps kill bacteria. *Science* **303,** 1532–1535
4. Papayannopoulos, V., Metzler, K. D., Hakkim, A., and Zychlinsky, A. (2010) Neutrophil elastase and myeloperoxidase regulate the formation of neutrophil extracellular traps. *J. Cell Biol.* **191,** 677–691
5. Borregaard, N., and Cowland, J. B. (1997) Granules of the human neutrophilic polymorphonuclear leukocyte. *Blood* **89,** 3503–3521
6. Cieutat, A. M., Lobel, P., August, J. T., Kjeldsen, L., Sengeløv, H., Borregaard, N., and Bainton, D. F. (1998) Azurophilic granules of human neutrophilic leukocytes are deficient in lysosome-associated membrane proteins but retain the mannose 6-phosphate recognition marker. *Blood* **91,** 1044–1058
7. Dahlgren, C., Carlsson, S. R., Karlsson, A., Lundqvist, H., and Sjölin, C. (1995) The lysosomal membrane glycoproteins Lamp-1 and Lamp-2 are present in mobilizable organelles, but are absent from the azurophil granules of human neutrophils. *Biochem. J.* **311,** 667–674
8. Tkalcevic, J., Novelli, M., Phylactides, M., Iredale, J. P., Segal, A. W., and

Roes, J. (2000) Impaired immunity and enhanced resistance to endotoxin in the absence of neutrophil elastase and cathepsin G. *Immunity* **12,** 201–210

9. Belaaouaj, A., McCarthy, R., Baumann, M., Gao, Z., Ley, T. J., Abraham, S. N., and Shapiro, S. D. (1998) Mice lacking neutrophil elastase reveal impaired host defense against gram negative bacterial sepsis. *Nat. Med.* **4,** 615–618

10. Kutter, D., Devaquet, P., Vanderstocken, G., Paulus, J. M., Marchal, V., and Gothot, A. (2000) Consequences of total and subtotal myeloperoxidase deficiency: risk or benefit ? *Acta Haematol.* **104,** 10–15

11. Babior, B. M. (1991) The respiratory burst oxidase and the molecular basis of chronic granulomatous disease. *Am. J. Hematol.* **37,** 263–266

12. Babior, B. M., and Woodman, R. C. (1990) Chronic granulomatous disease. *Semin. Hematol.* **27,** 247–259

13. Knaus, U. G., Heyworth, P. G., Kinsella, B. T., Curnutte, J. T., and Bokoch, G. M. (1992) Purification and characterization of Rac 2. A cytosolic GTP-binding protein that regulates human neutrophil NADPH oxidase. *J. Biol. Chem.* **267,** 23575–23582

14. Babior, B. M. (2004) NADPH oxidase. *Curr. Opin. Immunol.* **16,** 42–47

15. Sumimoto, H. (2008) Structure, regulation and evolution of Nox-family NADPH oxidases that produce reactive oxygen species. *FEBS J* **275,** 3249–3277

16. Matute, J. D., Arias, A. A., Wright, N. A., Wrobel, I., Waterhouse, C. C., Li, X. J., Marchal, C. C., Stull, N. D., Lewis, D. B., Steele, M., Kellner, J. D., Yu, W., Meroueh, S. O., Nauseef, W. M., and Dinauer, M. C. (2009) A new genetic subgroup of chronic granulomatous disease with autosomal recessive mutations in p40 phox and selective defects in neutrophil NADPH oxidase activity. *Blood* **114,** 3309–3315

17. Borregaard, N., Heiple, J. M., Simons, E. R., and Clark, R. A. (1983) Subcellular localization of the b-cytochrome component of the human neutrophil microbicidal oxidase: translocation during activation. *J. Cell Biol.* **97,** 52–61

18. Uriarte, S. M., Rane, M. J., Luerman, G. C., Barati, M. T., Ward, R. A., Nauseef, W. M., and McLeish, K. R. (2011) Granule exocytosis contributes to priming and activation of the human neutrophil respiratory burst. *J. Immunol.* **187,** 391–400

19. Ward, R. A., Nakamura, M., and McLeish, K. R. (2000) Priming of the neutrophil respiratory burst involves p38 mitogen-activated protein kinase-dependent exocytosis of flavocytochrome b_{558}-containing granules. *J. Biol. Chem.* **275,** 36713–36719

20. Jankowski, A., Scott, C. C., and Grinstein, S. (2002) Determinants of the phagosomal pH in neutrophils. *J. Biol. Chem.* **277,** 6059–6066

21. Suh, C. I., Stull, N. D., Li, X. J., Tian, W., Price, M. O., Grinstein, S., Yaffe, M. B., Atkinson, S., and Dinauer, M. C. (2006) The phosphoinositide-binding protein p40 phox activates the NADPH oxidase during FcγIIA receptor-induced phagocytosis. *J. Exp. Med.* **203,** 1915–1925

22. Tian, W., Li, X. J., Stull, N. D., Ming, W., Suh, C. I., Bissonnette, S. A., Yaffe, M. B., Grinstein, S., Atkinson, S. J., and Dinauer, M. C. (2008) FcγR-stimulated activation of the NADPH oxidase: phosphoinositide-binding protein p40 phox regulates NADPH oxidase activity after enzyme assembly on the phagosome. *Blood* **112,** 3867–3877

23. Tse, S. M., Furuya, W., Gold, E., Schreiber, A. D., Sandvig, K., Inman, R. D., and Grinstein, S. (2003) Differential role of actin, clathrin, and dynamin in Fcγ receptor-mediated endocytosis and phagocytosis. *J. Biol. Chem.* **278,** 3331–3338

24. Huynh, K. K., Eskelinen, E. L., Scott, C. C., Malevanets, A., Saftig, P., and Grinstein, S. (2007) LAMP proteins are required for fusion of lysosomes with phagosomes. *EMBO J.* **26,** 313–324

25. Tolmachova, T., Anders, R., Stinchcombe, J., Bossi, G., Griffiths, G. M., Huxley, C., and Seabra, M. C. (2004) A general role for Rab27a in secretory cells. *Mol. Biol. Cell* **15,** 332–344

26. Munafó, D. B., Johnson, J. L., Ellis, B. A., Rutschmann, S., Beutler, B., and Catz, S. D. (2007) Rab27a is a key component of the secretory machinery of azurophilic granules in granulocytes. *Biochem. J.* **402,** 229–239

27. Brzezinska, A. A., Johnson, J. L., Munafo, D. B., Crozat, K., Beutler, B., Kiosses, W. B., Ellis, B. A., and Catz, S. D. (2008) The Rab27a effectors JFC1/Slp1 and Munc13-4 regulate exocytosis of neutrophil granules. *Traffic* **9,** 2151–2164

28. Johnson, J. L., Brzezinska, A. A., Tolmachova, T., Munafo, D. B., Ellis, B. A., Seabra, M. C., Hong, H., and Catz, S. D. (2010) Rab27a and Rab27b regulate neutrophil azurophilic granule exocytosis and NADPH oxidase activity by independent mechanisms. *Traffic* **11,** 533–547

29. Pivot-Pajot, C., Varoqueaux, F., de Saint Basile, G., and Bourgoin, S. G. (2008) Munc13-4 regulates granule secretion in human neutrophils. *J. Immunol.* **180,** 6786–6797

30. Johnson, J. L., Hong, H., Monfregola, J., Kiosses, W. B., and Catz, S. D. (2011) MUNC13-4 restricts motility of RAB27A-expressing vesicles to facilitate lipopolysaccharide-induced priming of exocytosis in neutrophils. *J. Biol. Chem.* **286,** 5647–5656

31. Wood, S. M., Meeths, M., Chiang, S. C., Bechensteen, A. G., Boelens, J. J., Heilmann, C., Horiuchi, H., Rosthøj, S., Rutynowska, O., Winiarski, J., Stow, J. L., Nordenskjöld, M., Henter, J. I., Ljunggren, H. G., and Bryceson, Y. T. (2009) Different NK cell-activating receptors preferentially recruit Rab27a or Munc13-4 to perforin-containing granules for cytotoxicity. *Blood* **114,** 4117–4127

32. Ménasché, G., Pastural, E., Feldmann, J., Certain, S., Ersoy, F., Dupuis, S., Wulffraat, N., Bianchi, D., Fischer, A., Le Deist, F., and de Saint Basile, G. (2000) Mutations in RAB27A cause Griscelli syndrome associated with haemophagocytic syndrome. *Nat. Genet.* **25,** 173–176

33. Feldmann, J., Callebaut, I., Raposo, G., Certain, S., Bacq, D., Dumont, C., Lambert, N., Ouachée-Chardin, M., Chedeville, G., Tamary, H., Minard-Colin, V., Vilmer, E., Blanche, S., Le Deist, F., Fischer, A., and de Saint Basile, G. (2003) Munc13-4 is essential for cytolytic granules fusion and is mutated in a form of familial hemophagocytic lymphohistiocytosis (FHL3). *Cell* **115,** 461–473

34. Mahlaoui, N., Ouachée-Chardin, M., de Saint Basile, G., Neven, B., Picard, C., Blanche, S., and Fischer, A. (2007) Immunotherapy of familial hemophagocytic lymphohistiocytosis with antithymocyte globulins: a single-center retrospective report of 38 patients. *Pediatrics* **120,** e622–e628

35. Crozat, K., Hoebe, K., Ugolini, S., Hong, N. A., Janssen, E., Rutschmann, S., Mudd, S., Sovath, S., Vivier, E., and Beutler, B. (2007) Jinx, an MCMV susceptibility phenotype caused by disruption of Unc13d: a mouse model of type 3 familial hemophagocytic lymphohistiocytosis. *J. Exp. Med.* **204,** 853–863

36. Wilson, S. M., Yip, R., Swing, D. A., O'Sullivan, T. N., Zhang, Y., Novak, E. K., Swank, R. T., Russell, L. B., Copeland, N. G., and Jenkins, N. A. (2000) A mutation in Rab27a causes the vesicle transport defects observed in ashen mice. *Proc. Natl. Acad. Sci. U.S.A.* **97,** 7933–7938

37. Pollock, J. D., Williams, D. A., Gifford, M. A., Li, L. L., Du, X., Fisherman, J., Orkin, S. H., Doerschuk, C. M., and Dinauer, M. C. (1995) Mouse model of X-linked chronic granulomatous disease, an inherited defect in phagocyte superoxide production. *Nat. Genet.* **9,** 202–209

38. Liu, G. Y., Essex, A., Buchanan, J. T., Datta, V., Hoffman, H. M., Bastian, J. F., Fierer, J., and Nizet, V. (2005) *Staphylococcus aureus* golden pigment impairs neutrophil killing and promotes virulence through its antioxidant activity. *J. Exp. Med.* **202,** 209–215

39. Johnson, J. L., Monfregola, J., Napolitano, G., Kiosses, W. B., and Catz, S. D. (2012) Vesicular trafficking through cortical actin during exocytosis is regulated by the Rab27a effector JFC1/Slp1 and the RhoA-GTPase-activating protein Gem-interacting protein. *Mol. Biol. Cell* **23,** 1902–1916

40. Markert, M., Andrews, P. C., and Babior, B. M. (1984) Measurement of O_2^- production by human neutrophils. The preparation and assay of NADPH oxidase-containing particles from human neutrophils. *Methods Enzymol.* **105,** 358–365

41. Fuchs, T. A., Abed, U., Goosmann, C., Hurwitz, R., Schulze, I., Wahn, V., Weinrauch, Y., Brinkmann, V., and Zychlinsky, A. (2007) Novel cell death program leads to neutrophil extracellular traps. *J. Cell Biol.* **176,** 231–241

42. Li, Y., Karlin, A., Loike, J. D., and Silverstein, S. C. (2002) A critical concentration of neutrophils is required for effective bacterial killing in suspension. *Proc. Natl. Acad. Sci. U.S.A.* **99,** 8289–8294

43. Lin, J. S., Park, M. K., and Nahm, M. H. (2001) Chromogenic assay measuring opsonophagocytic killing capacities of antipneumococcal antisera. *Clin. Diagn. Lab. Immunol.* **8,** 528–533

44. Berridge, M. V., Herst, P. M., and Tan, A. S. (2005) Tetrazolium dyes as tools in cell biology: new insights into their cellular reduction. *Biotechnol. Annu. Rev.* **11,** 127–152

45. Green, S. P., Cairns, B., Rae, J., Errett-Baroncini, C., Hongo, J. A., Erickson, R. W., and Curnutte, J. T. (2001) Induction of gp91-phox, a component of the phagocyte NADPH oxidase, in microglial cells during central nervous system inflammation. *J. Cereb. Blood Flow Metab.* **21,** 374–384

46. Bedard, K., and Krause, K. H. (2007) The NOX family of ROS-generating NADPH oxidases: physiology and pathophysiology. *Physiol. Rev.* **87,** 245–313

47. Elstak, E. D., Neeft, M., Nehme, N. T., Voortman, J., Cheung, M., Goodarzifard, M., Gerritsen, H. C., van Bergen En Henegouwen, P. M., Callebaut, I., de Saint Basile, G., and van der Sluijs, P. (2011) The munc13-4-rab27 complex is specifically required for tethering secretory lysosomes at the plasma membrane. *Blood* **118,** 1570–1578

48. Mattheyses, A. L., and Axelrod, D. (2006) Direct measurement of the evanescent field profile produced by objective-based total internal reflection fluorescence. *J. Biomed. Opt.* **11,** 014006

49. Sengeløv, H., Nielsen, M. H., and Borregaard, N. (1992) Separation of human neutrophil plasma membrane from intracellular vesicles containing alkaline phosphatase and NADPH oxidase activity by free flow electrophoresis. *J. Biol. Chem.* **267,** 14912–14917

50. Boswell, K. L., James, D. J., Esquibel, J. M., Bruinsma, S., Shirakawa, R., Horiuchi, H., and Martin, T. F. (2012) Munc13-4 reconstitutes calcium-dependent SNARE-mediated membrane fusion. *J. Cell Biol.* **197,** 301–312

51. Lundqvist, H., and Dahlgren, C. (1996) Isoluminol-enhanced chemiluminescence: a sensitive method to study the release of superoxide anion from human neutrophils. *Free Radic. Biol. Med.* **20,** 785–792

52. Boxer, L. A., Yoder, M., Bonsib, S., Schmidt, M., Ho, P., Jersild, R., and Baehner, R. L. (1979) Effects of a chemotactic factor, *N*-formylmethionyl peptide, on adherence, superoxide anion generation, phagocytosis, and microtubule assembly of human polymorphonuclear leukocytes. *J. Lab. Clin. Med.* **93,** 506–514

53. Pacquelet, S., Johnson, J. L., Ellis, B. A., Brzezinska, A. A., Lane, W. S., Munafo, D. B., and Catz, S. D. (2007) Cross-talk between IRAK-4 and the NADPH oxidase. *Biochem. J.* **403,** 451–461

54. Schwartz, J., Leidal, K. G., Femling, J. K., Weiss, J. P., and Nauseef, W. M. (2009) Neutrophil bleaching of GFP-expressing staphylococci: probing the intraphagosomal fate of individual bacteria. *J. Immunol.* **183,** 2632–2641

55. Perskvist, N., Roberg, K., Kulyté, A., and Stendahl, O. (2002) Rab5a GTPase regulates fusion between pathogen-containing phagosomes and cytoplasmic organelles in human neutrophils. *J. Cell Sci.* **115,** 1321–1330

56. Vieira, O. V., Botelho, R. J., and Grinstein, S. (2002) Phagosome maturation: aging gracefully. *Biochem. J.* **366,** 689–704

57. Ménager, M. M., Ménasché, G., Romao, M., Knapnougel, P., Ho, C. H., Garfa, M., Raposo, G., Feldmann, J., Fischer, A., and de Saint Basile, G. (2007) Secretory cytotoxic granule maturation and exocytosis require the effector protein hMunc13-4. *Nat. Immunol.* **8,** 257–267

58. Gobor, T., Corol, G., Ferreira, L. E., Rymovicz, A. U., Rosa, R. T., Campelo, P. M., and Rosa, E. A. (2011) Proposal of protocols using D-glutamine to optimize the 2,3-bis(2-methoxy-4-nitro-5-sulfophenly)-5-[(phenyl-amino)carbonyl]-2*H*-tetrazolium hydroxide (XTT) assay for indirect estimation of microbial loads in biofilms of medical importance. *J. Microbiol. Methods* **84,** 299–306

59. Tunney, M. M., Ramage, G., Field, T. R., Moriarty, T. F., and Storey, D. G. (2004) Rapid colorimetric assay for antimicrobial susceptibility testing of *Pseudomonas aeruginosa. Antimicrob. Agents Chemother.* **48,** 1879–1881

60. Speert, D. P., Bond, M., Woodman, R. C., and Curnutte, J. T. (1994) Infection with Pseudomonas cepacia in chronic granulomatous disease: role of nonoxidative killing by neutrophils in host defense. *J. Infect. Dis.* **170,** 1524–1531

61. Neeft, M., Wieffer, M., de Jong, A. S., Negroiu, G., Metz, C. H., van Loon, A., Griffith, J., Krijgsveld, J., Wulffraat, N., Koch, H., Heck, A. J., Brose, N., Kleijmeer, M., and van der Sluijs, P. (2005) Munc13-4 is an effector of rab27a and controls secretion of lysosomes in hematopoietic cells. *Mol. Biol. Cell* **16,** 731–741

62. Marcenaro, S., Gallo, F., Martini, S., Santoro, A., Griffiths, G. M., Aricó, M., Moretta, L., and Pende, D. (2006) Analysis of natural killer-cell function in familial hemophagocytic lymphohistiocytosis (FHL): defective CD107a surface expression heralds Munc13-4 defect and discriminates between genetic subtypes of the disease. *Blood* **108,** 2316–2323

63. Ren, Q., Wimmer, C., Chicka, M. C., Ye, S., Ren, Y., Hughson, F. M., and Whiteheart, S. W. (2010) Munc13-4 is a limiting factor in the pathway required for platelet granule release and hemostasis. *Blood* **116,** 869–877

64. Kantonen, S., Hatton, N., Mahankali, M., Henkels, K. M., Park, H., Cox, D., and Gomez-Cambronero, J. (2011) A novel phospholipase D2-Grb2-WASp heterotrimer regulates leukocyte phagocytosis in a two-step mechanism. *Mol. Cell. Biol.* **31,** 4524–4537

65. Winter, J., Ilbert, M., Graf, P. C., Ozcelik, D., and Jakob, U. (2008) Bleach activates a redox-regulated chaperone by oxidative protein unfolding. *Cell* **135,** 691–701

66. Seto, S., Tsujimura, K., and Koide, Y. (2011) Rab GTPases regulating phagosome maturation are differentially recruited to mycobacterial phagosomes. *Traffic* **12,** 407–420

67. Yokoyama, K., Kaji, H., He, J., Tanaka, C., Hazama, R., Kamigaki, T., Ku, Y., Tohyama, K., and Tohyama, Y. (2011) Rab27a negatively regulates phagocytosis by prolongation of the actin-coating stage around phagosomes. *J. Biol. Chem.* **286,** 5375–5382

68. Zhang, S., Ma, D., Wang, X., Celkan, T., Nordenskjöld, M., Henter, J. I., Fadeel, B., and Zheng, C. (2008) Syntaxin-11 is expressed in primary human monocytes/macrophages and acts as a negative regulator of macrophage engulfment of apoptotic cells and IgG-opsonized target cells. *Br. J. Haematol.* **142,** 469–479

69. Munafo, D. B., Johnson, J. L., Brzezinska, A. A., Ellis, B. A., Wood, M. R., and Catz, S. D. (2009) DNase I inhibits a late phase of reactive oxygen species production in neutrophils. *J. Innate Immun.* **1,** 527–542

70. Nold-Petry, C. A., Lehrnbecher, T., Jarisch, A., Schwabe, D., Pfeilschifter, J. M., Muhl, H., and Nold, M. F. (2010) Failure of interferon γ to induce the anti-inflammatory interleukin 18 binding protein in familial hemophagocytosis. *PLoS One* **5,** e8663

71. Rohr, J., Beutel, K., Maul-Pavicic, A., Vraetz, T., Thiel, J., Warnatz, K., Bondzio, I., Gross-Wieltsch, U., Schündeln, M., Schütz, B., Woessmann, W., Groll, A. H., Strahm, B., Pagel, J., Speckmann, C., Janka, G., Griffiths, G., Schwarz, K., zur Stadt, U., and Ehl, S. (2010) Atypical familial hemophagocytic lymphohistiocytosis due to mutations in UNC13D and STXBP2 overlaps with primary immunodeficiency diseases. *Haematologica* **95,** 2080–2087